

Invited Feature Article

## Liquid Polyamorphous Transition and Self-Organization in Aqueous Solutions of Ionic Surfactants

Yuriy A. Mirgorod, and Tatiana A Dolenko

*Langmuir*, **Just Accepted Manuscript** • DOI: 10.1021/acs.langmuir.5b00479 • Publication Date (Web): 23 Mar 2015

Downloaded from <http://pubs.acs.org> on March 28, 2015

### Just Accepted

“Just Accepted” manuscripts have been peer-reviewed and accepted for publication. They are posted online prior to technical editing, formatting for publication and author proofing. The American Chemical Society provides “Just Accepted” as a free service to the research community to expedite the dissemination of scientific material as soon as possible after acceptance. “Just Accepted” manuscripts appear in full in PDF format accompanied by an HTML abstract. “Just Accepted” manuscripts have been fully peer reviewed, but should not be considered the official version of record. They are accessible to all readers and citable by the Digital Object Identifier (DOI®). “Just Accepted” is an optional service offered to authors. Therefore, the “Just Accepted” Web site may not include all articles that will be published in the journal. After a manuscript is technically edited and formatted, it will be removed from the “Just Accepted” Web site and published as an ASAP article. Note that technical editing may introduce minor changes to the manuscript text and/or graphics which could affect content, and all legal disclaimers and ethical guidelines that apply to the journal pertain. ACS cannot be held responsible for errors or consequences arising from the use of information contained in these “Just Accepted” manuscripts.



**Liquid Polyamorphous Transition and Self-Organization****in Aqueous Solutions of Ionic Surfactants**Yuriy A. Mirgorod<sup>a)</sup>, Tatiana A. Dolenko<sup>b)</sup><sup>a)</sup>South-West State University, 305040, Kursk, Russia<sup>b)</sup>Department of Physics, M.V.Lomonosov Moscow State University, Moscow, 119991, Russia

*Polyamorphous transitions in supercooled water, porous substances, solutions of polyols and proteins are studied intensively. They accompany self-organization of hydrocarbons and surfactants. In this study, the methods of polyamorphous transitions identification are proposed, their dependence on hydrocarbons and surfactants concentration and sizes is investigated. The place of polyamorphous transitions in the general theory of phase separation is determined, their bistability, self-oscillations, hysteresis, fluctuations, cooperative effect, enthalpy, entropy are described. Surface, volume and diffusion instabilities of polyamorphous transitions are analyzed. Technologies based on the properties of polyamorphous transitions are proposed.*

**INTRODUCTION**

Amorphous polymorphism (polyamorphism) is a key in modern conception of water structure, of physical properties and anomalies of water.<sup>1,2</sup> The main idea of this conception is the following: at ambient conditions, liquid water (with average density 1 g/cm<sup>3</sup>) fluctuates permanently between low-density liquid (LDL, density 0.94 g/cm<sup>3</sup>) and high-density liquid (HDL, density 1.14 g/cm<sup>3</sup>) clusters with size  $\approx 1$  nm.<sup>3</sup> Clusters cannot be allocated in water at ambient temperatures, but the phase separation between them may exist at temperatures below 233 K. The phase boundary should disappear in the critical point at a lower temperature. Such research can result in application of supercooled water as supercritical solvent. Experimental study of Liquid-Liquid Polyamorphous Transition (LLPT) is a complicated problem, because supercooled water at temperature below the temperature of homogeneous nucleation 235 K under 0.1 MPa spontaneously transforms to crystalline form. Difficulties of the experiments with supercooled water shift the

1  
2  
3  
4  
5  
6  
7  
8  
9  
10  
11  
12  
13  
14  
15  
16  
17  
18  
19  
20  
21  
22  
23  
evidence of LLPT existence to the domain of numerical modeling. Now this problem is discussed in literature intensively.<sup>4</sup>

To achieve deeper supercooling of water and to observe LLPT in it, indirect methods of studying supercooled water are used, for example, in hydrophobic and hydrophilic nanopores.<sup>5,6</sup> However, the surface of nanopores material influence LLPT essentially. In the other indirect method, to increase the temperature of homogeneous nucleation of ice, aqueous solutions of glycerin and other polyols are studied.<sup>7</sup> During LLPT in water-glycerin mixture there is no phase separation. It is the transition between liquid I and liquid II in supercooled state of solution with the same composition but with different density. Adding solute should generate a line of critical points liquid-liquid originating from the critical point of metastable water.<sup>8</sup> Therefore, the study of the LLPT in surfactant solutions and in other systems may shed light on LLPT in supercooled water.

24  
25  
26  
27  
28  
29  
30  
31  
32  
We assumed that LLPT accompanies a self-organization of non-electrolytes, inorganic electrolytes, surfactants in aqueous solutions at ambient conditions.<sup>9</sup> For electrolytes it begins when ion interaction is stopped and self-organization is determined only by the change of water activity,<sup>10</sup> i.e. by the change of its structure and by self-association.

33  
34  
35  
36  
37  
38  
39  
40  
41  
42  
43  
44  
45  
46  
47  
48  
49  
50  
51  
52  
53  
54  
55  
56  
57  
58  
59  
60  
LLPT accompanies the stabilization of biological structures,<sup>11</sup> the formation of spherical micelles of surfactants.<sup>12,13</sup> Micelles and micelle formation are studied for more than 100 years,<sup>14</sup> but yet in this area of knowledge much is not clear. Within the framework of the General theory of phase separation, micellization is studied poorly. It is usually considered that the critical concentration of micelle formation ( $CMC_1$ ) lies on a binodal. Then spherical micelles must be nucleus of macrophase, and the phase separation process should be accompanied by supersaturation. In fact, spherical micelles cannot be considered to be nucleus of a new phase, and supersaturation of surfactant in the area of  $CMC_1$  is not observed. It is believed that the sizes of spherical micelles of the most studied surfactant – sodium dodecyl sulfate (SDS) – are determined.<sup>14</sup> However, different methods determine different sizes of micelles. Static methods of SAXS and SANS show that micelles consist of 60-70 molecules,<sup>15</sup> while dynamic methods of NMR, DLS determine approximately 2 times less molecules.<sup>16</sup> In one homologous series of amphiphiles there is separation between hydrotrops and surfactants. The former are studied in physical chemistry of solutions, and the latter are studied in colloid

chemistry. It is unknown which of the homologs is the boundary between them, and what is the difference between self-organizing structures of these two kinds of diphilic electrolytes.

It is recognized that the gain in the Gibbs energy of micelle formation is caused by an increase of entropy during "melting of microicebergs" around hydrocarbon groups of surfactants<sup>14</sup>, but the phenomenon of "melting of microicebergs» (LLPT) has not yet been investigated. This is due to the difficulty in identifying LLPT by modern physical methods. In addition, micellization of surfactants is well explained by the phenomenological theory of hydrophobic interaction<sup>14</sup> and by the concept of potential of mean force<sup>17,18</sup> and, according to some authors, requires no additional approaches. In the kinetics of the micelle formation there is a problem of correspondence of relaxation processes to self-organizing structures.<sup>19</sup> The self-oscillations on the boundary of phase separation of nitrobenzene/solutions of ionic surfactants,<sup>20</sup> octanol/solutions of surfactants with additives of barbiton have been ascertained.<sup>21</sup> The authors of these studies do not associate the oscillations on the boundary of phases with self-oscillations in solution volume, although the relationship of surface and volume properties of surfactants solutions are well known.

Thus, without using the concept of LLPT, it is impossible to integrate micellization into a unified theory of phase separation, to explain the above mentioned contradictions, and to use surfactant in new technologies.

In this paper the studies of the authors on the role of LLPT in the processes of amphiphiles self-organization, partially explaining these and other problems, are summarized. First, LLPT will be considered in solutions of hydrocarbons, which, as in the study of hydrophobic interaction between surfactants, act as models. Then similar problems will be studied in solutions of amphiphiles depending on their concentration and length of the chain. After that we will proceed to the consideration of LLPT peculiarities and instabilities in solutions of surfactants, and we will finish with the description of possible directions of practical applications derived from the basic concept of LLPT.

## 1. POLYAMORPHOUS TRANSITIONS IN BINARY SYSTEMS N-HYDROCARBON-WATER

### 1.1. Hydrophobic hydration. Small water systems.

1  
2  
3  
4  
5  
6  
7  
8  
9  
10  
11  
12  
13  
14  
15  
16  
17  
18  
19  
20  
21  
22  
23  
24  
25  
26  
27  
28  
29  
30  
31  
32  
33  
34  
35  
The study of the density of aqueous solutions of non-electrolytes and ionic amphiphiles at 303 K showed that the partial volume of methylene groups at infinite dilution is equal to  $\Delta V_{CH_2} = -16.1 \cdot 10^{-6} \text{ m}^3 \cdot \text{mol}^{-1}$ . The minus sign indicates that the volume of methylene group in water is less than that in hydrocarbon for the value  $\Delta V_{CH_2}$ . The change in volume is due to rearrangement of water molecules around hydrocarbon radicals of non-electrolytes. This phenomenon is called hydrophobic hydration.<sup>22</sup> In the process of dissolution, hydrocarbon molecules "push out" water molecules to form a cavity. This combination of water molecules will be called a small system. A small system around the molecules of tert. butyl alcohol contains 15-17 water molecules,<sup>23</sup> which corresponds to the size of a molecule of alcohol. Reorientation time of water molecules in a small system is 4 times less than that in water volume.<sup>24</sup> C. Petersen calls small system of water molecules hydration shell, and H. Tanaka - locally favoured structures.<sup>10</sup> For a small system, the equivalence of mass and energy related with space and time is preserved, it is important to emphasize this for peculiarity of LLPT. The volumes of small systems fluctuate up to 40 % in certain periods of time.<sup>13</sup> In the layer around a hydrocarbon molecule, there can be more molecules of water than in the cavity. Part of them are from continuous network of H-bonds between the "non-displaced" molecules, but only molecules of the cavity will "work" in the processes, because they determine the equivalence of mass and energy in these processes. They represent the average in the distribution of molecules in a small system.

36  
37  
38  
39  
40  
41  
42  
43  
44  
45  
46  
47  
48  
Large negative changes of the enthalpy of dissolution and entropy of hydration of hydrocarbons and large negative changes in their partial molar volumes are evidence of formation of small water systems around the molecules of hydrocarbons. Explanation of mixing of two liquids, based on the dissolution of hydrocarbon, is in conflict with the positive sign of Gibbs energy in spontaneous process and absence of supersaturation of hydrocarbons during phase separation. The concept of LLPT proposed in this paper removes this contradiction.

49  
50  
51  
52  
53  
54  
55  
56  
57  
58  
59  
60  
Formation of small systems increases the solubility of hydrocarbons compared to the trend of solubility, starting from 373 K, when small systems are not formed.<sup>25</sup> Enthalpy of dissolution of hydrocarbons in water at a temperature higher than 100°C has a large positive value when formation of small systems becomes insignificant. It gradually decreases with temperature due to negative enthalpy of formation of small systems from the surrounding water molecules. Small and negative enthalpy of dissolution of

hydrocarbons at room temperature is the result of a large positive enthalpy of mixing (reduction of intermolecular interaction of neighboring molecules) and large negative enthalpy of formation of small systems.

Function of solubility  $x_2(T)$  for all n-hydrocarbons reaches a minimum at temperature  $T_{min} = 303$  K.<sup>22</sup> Like those for amphiphiles and many other non-electrolytes, this function wonderfully repeats the form of the dependence of isothermal compressibility  $\beta_T$  of water on temperature. When temperatures  $T_{min}$  coincide, a proportional relationship between  $lg(x_2)$  of hydrocarbons and  $1/\beta_T$  of water is observed. The Gibbs energy  $\Delta G_s^0$  of dissolution of hydrocarbon can be expressed by the following equation<sup>22</sup>:

$$\Delta G_s^0 = \mu_2^*(T, P) - \mu_2^{\circ}(T, P) = -RT \ln x_2, \quad (1)$$

Gibbs energy of formation of small system around hydrocarbon is equal to  $V/\beta_T$ , where  $V$  is the volume of small system at LLPT. Therefore, the functions of  $lg(x_2)$  and  $1/\beta_T$  are proportional, and confirm the concept of LLPT. The presence of hydrocarbons in water on binodal and spinodal shifts the minimum of  $\beta_T(T)$  of water and balance of LDL  $\leftrightarrow$  HDL, which was in water, up to 303 K.

Water is a good standard,<sup>22</sup> because the intensity of its small-angle x-ray scattering at  $q = 0.1 - 4$  nm<sup>-1</sup> depends on  $\beta_T$  only and it does not depend on the angle of the incident beam:

$$I_{H_2O}^{theory} = \rho^2 k_B T \beta_T, \quad (2)$$

where  $\rho$  is the scattering length density of water,  $k_B$  is the Boltzmann constant,  $T$  is temperature. The scattering length density (cm<sup>-2</sup>) of small system of water:  $\rho = (1/V) \sum_j b_j$ , where  $V$  is the volume of small system,  $b$  is the length of scattering. The length of the scattering is a stochastic function of element. For x-ray radiation it is linearly dependent on the number of element electrons. Therefore, with decrease of  $\beta_T$  the electron density of water clusters is decreased. Water becomes loose with the structure of LDL. With increase of  $\beta_T$  the electron density of water is increased. It builds up the content of structures of HDL.

Thus, by change of  $\beta_T$  of aqueous solutions and according to modern data on water microstructure, one can judge about the molecular organization of the ensemble of small systems.

## 1.2. Enthalpies of polyamorphous transitions in systems of water-hydrocarbon

Hydrocarbons and water are distributed within each other in small quantities. Solubility of hexane in water is  $x_2=2.21 \cdot 10^{-6}$  mole fraction, and the solubility of water in hexane is  $6.21 \cdot 10^{-3}$  mole fraction. Equilibrium at stirring of hydrocarbon in water excess is achieved in 40 hours. Low solubility is the main obstacle in the study of solutions of water and hydrocarbons. This is also the reason of the positive value of the Gibbs energy of dissolution.<sup>22</sup> Having the dependence of solubility on temperature, one can get the enthalpy of dissolution  $\Delta H_s^0$ , and using the enthalpy of evaporation  $\Delta H_{vap}$  one can calculate the enthalpy of hydrophobic hydration  $\Delta H_h^0$ .

Table 1. The thermodynamic functions of the dissolution of hydrocarbons and the enthalpy of polyamorphous transition in water

Hydrocarbon	$\Delta G_s^0$ , kJ•mole <sup>-1</sup>	$-\Delta H_h^0$ , kJ•mole <sup>-1</sup>	$-\Delta S_h^0$ , kJ•mole <sup>-1</sup>	$-\Delta H_{ph.tr}^0$ , kJ•mole <sup>-1</sup>
Butane	-	26.0	176.3	5.0
Pentane	28.6	28.4	188.7	4.9
Hexane	32.5	31.5	197.7	4.8

In Table 1, the enthalpy of hydrophobic hydration is calculated for 1 mole of alkane. To calculate enthalpy of polymorphous transition it is necessary to calculate this value for 1 mole of water.<sup>22</sup> To do this, we need to determine the number of water molecules removed from the cavity in the network of H-bonds of water to place hydrocarbon. To calculate the number of water molecules, the density of light ice 0.94 g/cm<sup>3</sup>, volume of CH<sub>3</sub> 0.0543 nm<sup>3</sup>, volume of CH<sub>2</sub> 0.0248 nm<sup>3</sup> will be used. As can be seen from Table 1, the enthalpies of polymorphous transition  $-\Delta H_{ph.tr}^0$  for three hydrocarbons differ little, within  $4.90 \pm 0.07$  kJ•mole<sup>-1</sup>. The obtained value of enthalpy of LLPT is between those for polymorphous modifications of ice.

The enthalpy of water dissolution in hydrocarbon can be also calculated, but using the dependence of water dissolubility on temperature. Unlike the enthalpy of hydrocarbons dissolution in water, it is positive and it is the same for all alkanes:  $34 \pm 1.4$  kJ•mole<sup>-1</sup>. This value is approximately equal to the energy of H-

bonds broken in water, 20-40 kJ•mole<sup>-1</sup>, i.e. it characterizes a phase transition that is like evaporation. Similar calculations are made for alcohols.<sup>22</sup>

Thus, the molecules of n-hydrocarbons in water excess in states to the left of binodal influence the ensembles of water small systems like temperature decrease (crystallization). From binodal to spinodal they influence like temperature increase (melting). "Crystallization" must be understood as the reduction of the reorientation time of water molecules in the ensemble of small systems, and "melting" must be understood as the return of water molecules to the previous state. In their excess, n-hydrocarbons break H-bonds of the whole network of water and effect water like temperature increase.

### 1.3. Dependence of polyamorphous transitions on the chain length and on the concentration of hydrocarbons

The phase diagram of hydrocarbons in the coordinates  $lg(x_2)(n)$  is presented in Figure 1.<sup>12</sup> It is discrete along the chain, and it is continuous along the concentration. The function  $lg(x_2)(n)$  for gaseous hydrocarbons C1-C4 has other slope in comparison with liquid hydrocarbons, because there is transfer of molecules from gas into water. This process is accompanied by unfavorable change of increment<sup>26</sup>  $\Delta G_{CH_2}^0 = +0.7$  kJ•mole<sup>-1</sup> ( $\Delta H^0_{CH_2} = -2.9$  kJ•mole<sup>-1</sup>,  $T\Delta S^0_{CH_2} = -3.6$  kJ•mole<sup>-1</sup>) (Figure 2). Molecules C1-C4 are placed in hollow space of tetrahedral network of water H-bonds like a formation of crystalline clathrates. The same thing happens in solutions of hydrotrops of s-alkylisothiuronium chloride (ATC). The slopes of  $lg(x_2)(n)$  of hydrocarbons and of  $lg(CPMC)(n)$  of ATC (binodales) are equal (Figure 1). According to our concept, hydrocarbons and hydrotrops are placed in the structure of LDL, shifting the balance in its direction. Calculations show that the size of the structure of LDL 1nm and butane correspond to the process.<sup>27</sup> Hydrocarbons C1-C4 have no phase separation between the solution and the hydrocarbon. So there is no spinodal.

For C5-C11, binodal and spinodal coincide, and they are the functions  $lg(x_2)$ , which are proportional to the Gibbs energies of dissolution. Solubility of hydrocarbons C11-C18 already does not follow this regularity.<sup>28</sup> At higher concentration, spinodal appears, and on the binodal a balance between LDL and HDL clusters is shifted to LDL maximally. By increasing concentration, molecules of C11-C18 hydrocarbons are "pushed out" by formed clusters of LDL in the process of LLPT to "micelles", which are the fluctuations of



the concentration before spinodal. Crystalline C20-C28 have a similar slope of the spinodal in the phase diagram. As the solubility of C20-C28 is greater than that of C11-C18, it is possible to assume the existence of microcrystals before spinodal (the border of absolute instability of the homogeneous system).

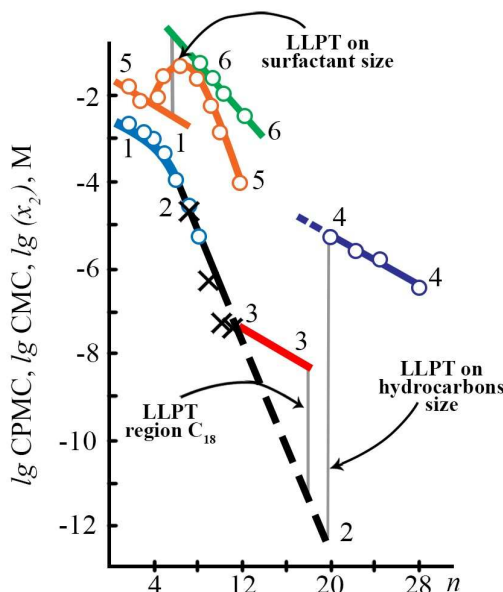


Figure 1. Phase diagrams of n-hydrocarbons and of s-alkylisothiuronium chlorides. 1,1 - solubility, binodal of gases of hydrocarbons C1-C4; 2,2 - solubility, binodal and spinodal of hydrocarbons; C5-C11; 3,3 - micellar solubility, spinodal of hydrocarbons C11-C18; 3,2- solubility, binodal of hydrocarbons C11-C18; 4,4 - micellar solubility, binodal of hydrocarbons C19-C28; 5,5 – critical pre-micelle concentration (CPMC), binodal of C2-C12 of s-alkylisothiuronium chlorides; 6,6 - CMC<sub>1</sub>, spinodal of C7-C12 of s-alkylisothiuronium chlorides.

Thermodynamic cycle of self-organization of hydrocarbons is similar to thermodynamic cycle of hydrated hydrophobic interaction of surfactants (Figure 2).<sup>28</sup> Increment of dissolution of alkanes C5-C18  $\Delta G^0_{CH_2}$  is equal to  $3.7 \text{ kJ}\cdot\text{mole}^{-1}$  ( $\Delta H^0_{CH_2} = 2.7 \text{ kJ}\cdot\text{mole}^{-1}$ ,  $T\Delta S^0_{CH_2} = -1.6 \text{ kJ}\cdot\text{mole}^{-1}$ ). Maximum hydrophobic hydration of C5-C11 occurs when the concentration is on binodal. At this boundary the transition from complete hydrophobic hydration ( $0.7 \text{ kJ}\cdot\text{mole}^{-1}$ ) to the border of complete hydrophobic dehydration ( $-0.7 \text{ kJ}\cdot\text{mole}^{-1}$ ) begins for hydrocarbons C11-C18 (dotted line in Figure 1), i.e. to hydrophobic interaction. Gibbs energy of the system decreases:  $\Delta G^0_{CH_2} = -1.4 \text{ kJ}\cdot\text{mole}^{-1}$ , which corresponds to "clean" intermolecular hydrophobic interaction. The gain in energy of association due to "net" hydrophobic

interaction is  $\Delta G_{\text{CH}_2}^0 = -0.7 \text{ kJ}\cdot\text{mole}^{-1}$  (Figure 2). The “net” or water-separated hydrophobic interaction includes association of methylene groups when they are separated by at least one layer of water molecules.<sup>26</sup> This process may occur if methylene groups change their state from hydrophobic hydration ( $\Delta G_{\text{CH}_2}^0 = +0.7 \text{ kJ}\cdot\text{mole}^{-1}$ ) to the state when water surrounding the methylene groups changes its structure ( $\Delta G_{\text{CH}_2}^0 = -0.7 \text{ kJ}\cdot\text{mole}^{-1}$ ) by LLPT. Taking into account the energy parameters of this process ( $\Delta H_{\text{CH}_2}^0 = 5.8 \text{ kJ}\cdot\text{mole}^{-1}$  and  $T\Delta S_{\text{CH}_2}^0 = 7.2 \text{ kJ}\cdot\text{mole}^{-1}$ ), it is possible to speak about weakening of H-bonds and increase of entropy of water without any contribution of the dispersion interaction.

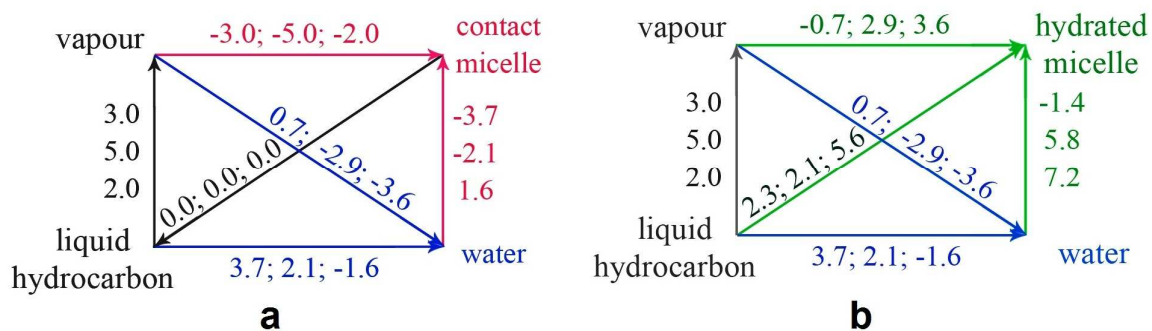


Figure 2. Thermodynamic cycles of  $\Delta G_{\text{CH}_2}^0$ ,  $\Delta H_{\text{CH}_2}^0$ ,  $T\Delta S_{\text{CH}_2}^0$  ( $\text{kJ}\cdot\text{mole}^{-1}$ ) of processes of dissolution in water, of evaporation, of hydrocarbon hydration, migration of hydrocarbon from vapour and water in micelles: contact hydrophobic (a) and hydrated hydrophobic (b) interaction.

Thus, in solutions of hydrocarbons C1-C4 on binodal, and C5-C11 on binodal and spinodal (which coincide) there is a sharp LLPT with enthalpy equaled to  $4.90 \pm 0.07 \text{ kJ}\cdot\text{mole}^{-1}$ . In solutions of C11-C18, LLPT is “stretched” over concentration between binodal and spinodal of the metastable region. The metastable region of C19-C28 increases even more. Undecane has critical size. Its binodal and spinodal touch, this corresponds to the critical point on the classical curve of phase separation.

## 2. POLYAMORPHOUS TRANSITIONS AND SELF-ORGANIZATION IN AQUEOUS SOLUTIONS OF AMPHIPHILES.

### 2.1. Theoretical model of polyamorphous transition

In macroscopic heterogeneous systems, the phase transition order-disorder (ice-water) can occur under such a small change of disturbing variable ( $T$ ) that any measurements in the transition region are practically impossible. The transition between two states in this case is a manifestation of maximum cooperativity.

In the ensemble of small systems, the transition between two states of water occurs under the final change of disturbing variable (the concentration of ions, molecules, effective internal pressure). This allows to carry out the equilibrium measurements of chemical and physical parameters in the transition region. Description of phase transitions in a system with a finite number of particles has not been sufficiently developed up to the present time.<sup>29</sup> As the theoretical basis of LLPT the thermodynamics of small systems and the transition between two states of T.Hill<sup>30,31</sup> was chosen.

The small system is a set of  $n$  of water molecules surrounding organic ion of amphiphile. Let's consider the ensemble of  $N$  of small systems with variables  $n, p, T$ , where  $n, p, T$  are the number of water molecules in small system, pressure and temperature, accordingly. Each small system in the proposed model can be in the state A, when its water molecules have less density of LDL, or in the state B, when water molecules have a high density of HDL. This assumption is justified by the increase of entropy of water during micellization of surfactants, by the existence of small systems with different densities in ambient water and by increase of  $\beta_T$  of amphiphiles water solutions after binodal. Now it is not yet possible to give the accurate description of the structure of small systems in positions A and B.

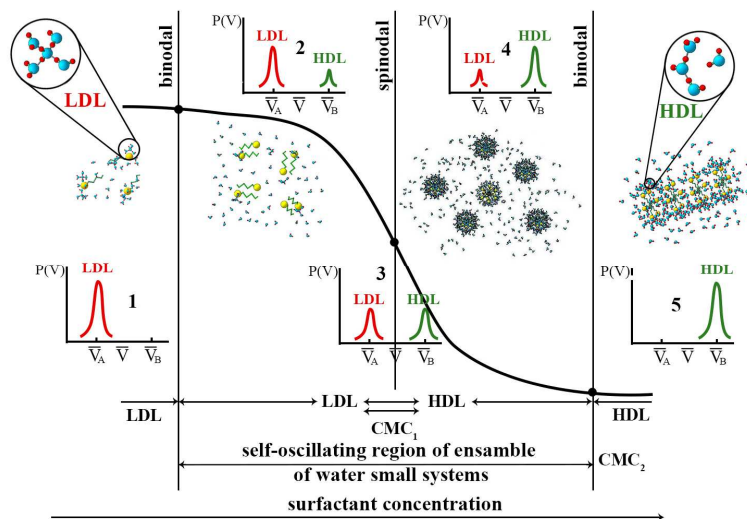


Figure 3. Polyamorphous transition in the ensemble of water small systems and self-organization of surfactant. Smooth change in the properties of water and self-oscillating region of water small systems between two binodal with increasing concentration of the amphiphile. 1 - the probability of volumes of water small system in the state A before the first binodal (CPMC); 2 - the probability of volumes of water small system in the state A and B between the first binodal and spinodal ( $CMC_1$ ), 3 - the probability of volumes of water small system in the state A and B on the spinodal ( $CMC_1$ ); 4 - the probability of volumes of water small systems in the state A and B between the spinodal and the second binodal ( $CMC_2$ ); 5 - the probability of volumes of water small system in the state B behind the second binodal ( $CMC_2$ ).

During LLPT a small system has a volume corresponding either to the state A  $\bar{V}_A$ , or to the state B  $\bar{V}_B$  (Figure 3). The size of the fluctuations around these values depends on the size of the small system. The probability of intermediate values of  $V$ , for example,  $V = \bar{V}$ , is insignificant. During LLPT in a small system a surface of the separation between A and B should be not exist. Otherwise in the ensemble unfavorable Gibbs energy of the surface appears. Therefore, the transition region is considered as a composition of two simple conditions A and B. The ensemble of small systems oscillates between states A and B due to the properties of the system itself. Extensive thermodynamic parameters of the ensemble of small systems in the transition region are linear combinations of thermodynamic parameters of the ensemble in states A and B. For example,  $(\partial G / \partial p)_{N,T} = \bar{V} = p_A \bar{V}_A + p_B \bar{V}_B$ , where  $G$  is the Gibbs energy of the ensemble of  $N$ ,  $\bar{V}$  is probability of intermediate values  $V$  of small system;  $p_A = N_A / N$  is the probability of the system to be in position A,  $p_B = 1 - p_A$  is the probability of a system to be in position B. Similarly, one can come to the chemical potential of small systems of water:  $(\partial G / \partial N)_{p,T} = \mu = p_A \mu_A + p_B \mu_B$ .

In the result of theoretical analysis of LLPT in the ensemble of small water systems one can make the following conclusions. The transition is significantly “stretched” with the concentration. In LLPT the middle of the transition can be identified. The ensemble of small systems during LLPT oscillates between two states A and B. Extensive thermodynamic parameters of the small system and of the ensemble of small systems fluctuate significantly.

## 2.2. Dependence of polyamorphous transition on the concentration of amphiphile

Let's consider the dependence of chemical potential of one of the components (hydrocarbon, amphiphile) on system composition in the framework of the general theory of phase separation.<sup>32</sup> System from a single-phase state AB to another single-phase state EF can transfer in three ways (Figure 4).

The first way is the formation of embryos of crystals (liquid) on binodal B in metastable state BC with nucleation kinetic. Binodal is the boundary between stable and metastable states of the system.

The second mechanism of phase separation occurs when the system has reached the spinodal C.

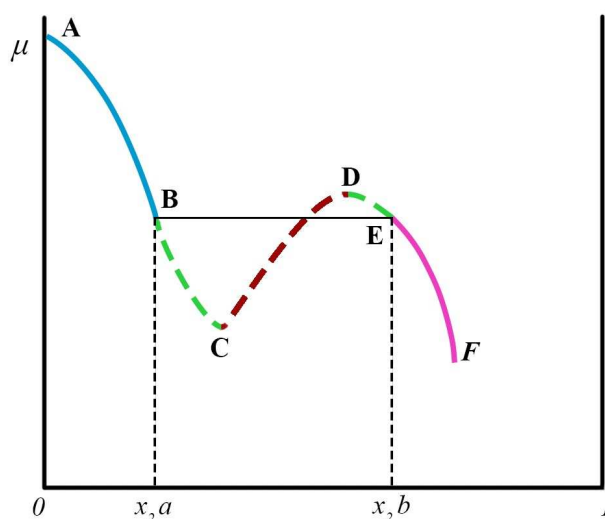


Figure 4. Dependence of chemical potential of one of the component  $a$  on system composition  $a+b$  in the framework of the general theory of phase separation. AB - single-phase state, EF-another single-phase state; BC, DE - metastable states, CD-unstable state, BE - two-phase state.

Spinodal is the boundary between stable (metastable) and unstable states of the homogeneous system. For hydrocarbons C5 to C11 (Figure1), concentrations of binodal B (Figure 4) and of spinodal C coincide. The unstable state of the system between C and D is characterized by the condition  $\partial\mu_2/\partial x_2 < 0$ . Spinodal decomposition (phase transition with participation of unstable states) has no directed flows of mass and energy, and characteristic times of decomposition of the double liquid systems are small. Formed structures rapidly decay, and phase separation realized. In alloys, polymer mixtures structure of spinodal decay freezes.

1  
2  
3  
4  
5  
6  
7  
8  
9  
10  
11  
12  
13  
14  
15  
16  
17  
18  
19  
20  
21  
22  
23  
24  
25  
26  
27  
28  
29  
30  
31  
32  
33  
34  
35  
36  
37  
38  
39  
40  
41  
42  
43  
44  
45  
46  
47  
48  
49  
50  
51  
52  
53  
54  
55  
56  
57  
58  
59  
60

Murata and Tanaka<sup>7</sup> have argued that the formation of a more stable liquid phase in supercooled aqueous solutions of glycerol may occur by two alternative types of kinetics: nucleation and spinodal decomposition. The concentrations of spinodals and binodals of ionic amphiphiles differ significantly (Figure 1).

The third type of self-organization arises when directed flows of mass and (or) energy are present. In this case, the formation of the new structure, starting from the spinodal, occurs only in conditions of irreversibility and energy dissipation. The system via unstable states transfers to a new stable state of dissipative structure.

In systems of water - surfactants the phase separation occurs according to the fourth scenario. The supersaturation of surfactant in system cannot be achieved, because there is not enough space to place large molecules of amphiphiles in network of water H-bonds. In metastable state BC (Figure 4) in the system water - surfactants with  $n > 7$  the balance between small systems LDL and HDL is shifted to LDL. This fact is proved by us using jump of  $\beta_T$  in solution of sodium dodecyl sulfate (SDS)  $2 \cdot 10^{-4}$  mole  $l^{-1}$ , with a minimum of  $44.8 \text{ Pa}^{-1}$ .<sup>33</sup> Metastable state (CPMC) in the solution of SDS on BC is fixed by different methods in region from  $2 \cdot 10^{-4}$  up to  $10^{-3}$  mole  $l^{-1}$ . Formation of small systems on binodal (CPMC) is very sensitive to impurities that can be both in water and in surfactants. Therefore, there is a large variance of concentration (on binodal) of SDS, around which small water systems are formed. More so that the concentrations are determined by different methods. On binodal the beginning LLPT is accompanied by the formation of dimers, i.e. premicells that prepare micellization.<sup>34</sup> However, dimers cannot be regarded as classic nucleuses of phase, because they are formed in results of "net" hydrophobic interactions (Figure 2, b). Then from C to B  $\beta_T$  of SDS increased from  $44.8 \cdot 10^{-11} \text{ Pa}^{-1}$  to  $60 \cdot 10^{-11} \text{ Pa}^{-1}$ , not reaching  $\text{CMC}_1$ . The similar behavior is observed for solution of cetylpyridinium chloride (CPC) (see Figure 10). At low  $\beta_T$  water ensemble of small systems of water becomes loose, with the structure of LDL. With increase of  $\beta_T$  the electron density of water increases. It increases the content of HDL structure (see Figures 6,7).

The phase separation of amphiphiles is similar to the third scenario. However, this scenario develops without external energy. In result of dissolution of new portions of amphiphiles due to hydrophilic groups the LLPT begins on binodal.

1  
2  
3  
4  
5  
6  
7  
8  
9  
10  
11  
12  
13  
14  
15  
16  
17  
18  
19  
20  
21  
22  
23  
The macrosystem can be heterogeneous (ice-water). The soft small system cannot be heterogeneous, since unfavorable Gibbs energy of surface appears, and the phase transition will not be gainful. Therefore, at the LLPT the ensemble of small water systems is a composition of the states A and B with their statistical weights. In the middle of LLPT ( $CMC_1$ , spinodal), statistical weights of the states A and B are equal (Figure 3). This state is unstable, as in a small system with an interface. The concentrations of spinodals C and D (Figure 4) are approximately equal. Due to the special properties of LLPT, the system overcomes the spinodal and the unstable state (Figure 4). Micelles of hydrocarbons (concentration fluctuations) C11-C18 and C19-C28 are formed in a metastable state BC. The idea, known as “water’s polyamorphism”, hypothesizes that the phase separation and possible existence of two alternative macrostructures with different densities in supercooled liquid water is similar to LLPT and differs from our LLPT.<sup>35</sup> Our transition occurs only in the presence of amphiphiles and depends on the size and concentration of the amphiphiles.

24  
25  
26  
27  
28  
29  
30  
31  
32  
33  
34  
We have found that using measurements of pH of aqueous solutions of ATC, one can follow the changes of state of the ensemble of small water systems around molecules amphiphiles (Figure 5).<sup>12,33</sup> In aqueous solution ATC dissociates. The positive charge of hydrophilic group is distributed on two atoms of nitrogen, sulfur and carbon. Such distribution of the charge gives the special properties to this surfactant in comparison with others. There is almost no thermal effect when solution is diluted.

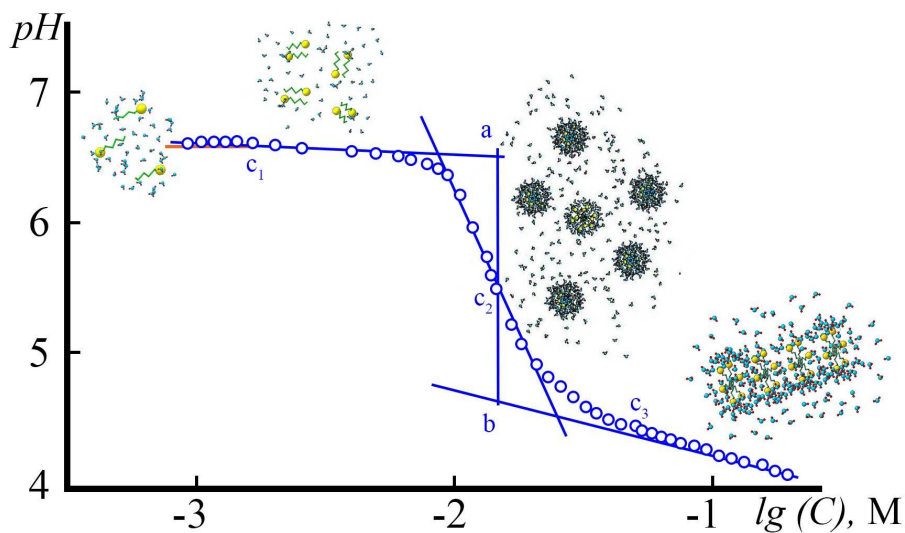
35  
36  
37  
38  
39  
40  
41  
42  
43  
44  
45  
46  
47  
48  
49  
50  
The first specific point on the curve  $pH(-lgc)$  of ATC at low concentrations corresponds to the true solubility without the association by hydrocarbon groups, i.e. hydrophobic interaction. Reaching this concentration small systems begin to change its structure because network of H-bonds of water can not place new molecules of surfactants. The formation of dimmers begins. This concentration lies on binodal. One can speak about maximum shift of the balance to LDL in comparison with water. Therefore, LLPT begins. At concentration  $CMC_1$  spherical micelles formed. This particular point coincides with spinodal. When the concentration  $CMC_2$  was reached micelles of cylindrical shape are formed.

51  
52  
53  
54  
55  
56  
57  
58  
59  
60  
We believe that this particular point lies on binodal when there are no water molecules that have the opportunity to participate in LLPT and self-organization of amphiphiles is determined by the concept of geometrical packing.<sup>14</sup> The other water molecules connected with hydrophilic group of amphiphile more strongly. Functions  $CMC_1(T)$  and  $CMC_2(T)$  have the opposite extremes. The first function has minimum, and

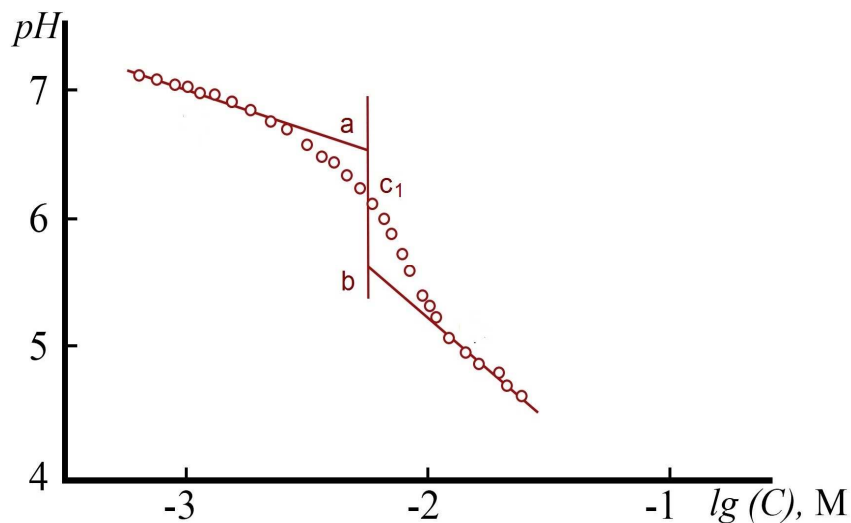
the second one has maximum like to the lower and upper critical points in the classical phase separation.<sup>36</sup>

Apparently,  $CMC_2$  is a maximum concentration of water allocation in phase of surfactant.

Thus, the middle part of LLPT corresponds to  $CMC_1$ . Values of  $CMC_1$  of ATC, determined using conductivity, surface tension and pH approximately coincide.<sup>37</sup>



a



b

Figure 5. Dependence of polyamorphous transition on the concentration of amphiphile. The dependences of pH on logarithm of the concentration of s-decylisothiuronium chloride (a) and s-hexylisothiuronium chloride (b) in aqueous solution at 25°C.  $C_1$  is the beginning of the transition (the beginning of formation of pre-micelles),  $C_2$  is the middle of LL-transition ( $CMC_1$ ),  $C_3$  is the completion of transition ( $CMC_2$ ), ab is the "depth" of the transition.



1  
2 The degree of cooperativity of LLPT  $dlg(a(H^+))/dlgc$  (where  $lg(a(H^+))$  is the negative logarithm of  
3 activity of ATC or pH) in the middle part increases proportionally to the increase of  $n$ , i.e. to the size of the  
4 small water system. Similar dependence is observed between changes of pH in the middle part of LLPT  
5 (depth of the transition) and of the size of a small system.<sup>37</sup>  
6  
7  
8  
9

10 One can discover LLPT by the self-diffusion coefficient of water in aqueous solutions of sodium para-  
11 octylbenzolsulphonate,<sup>38</sup> by the dependence of water activity on the concentration of sodium octanoate,<sup>39</sup> by  
12 the dependence of rate of proton magnetic relaxation of water on the total concentration of ammonium salt of  
13 perfluoro-2-methyl-3-oxihexanoic acid,<sup>40</sup> by thermal effect of the dissolution of SDS. The researchers, who  
14 obtained these results, did not pay attention to LLPT.<sup>41</sup>  
15  
16  
17  
18  
19  
20  
21

22 Different methods of LLPT study give different results. Thus, using water activity in the solutions of  
23 sodium octanoate, one can get the same s-function as in Figure 5. Using the thermal effect of the dissolution  
24 of crystalline SDS one can get two s-functions. Dissolution at lower concentrations is characterized by the  
25 change of enthalpy  $\Delta H_s^0 = 1 \text{ kJ mole}^{-1}$ , and at greater concentrations -  $\Delta H_s^0 = 2 \text{ kJ mole}^{-1}$ . The stage at the  
26 lower concentration is accompanied by formation of pre-micelles in the solution, what is a preparatory stage  
27 of LLPT before the formation of spherical micelles when reaching  $CMC_1$  with  $\Delta H_s^0 = 2 \text{ kJ mole}^{-1}$ .  
28  
29  
30  
31  
32  
33  
34  
35  
36

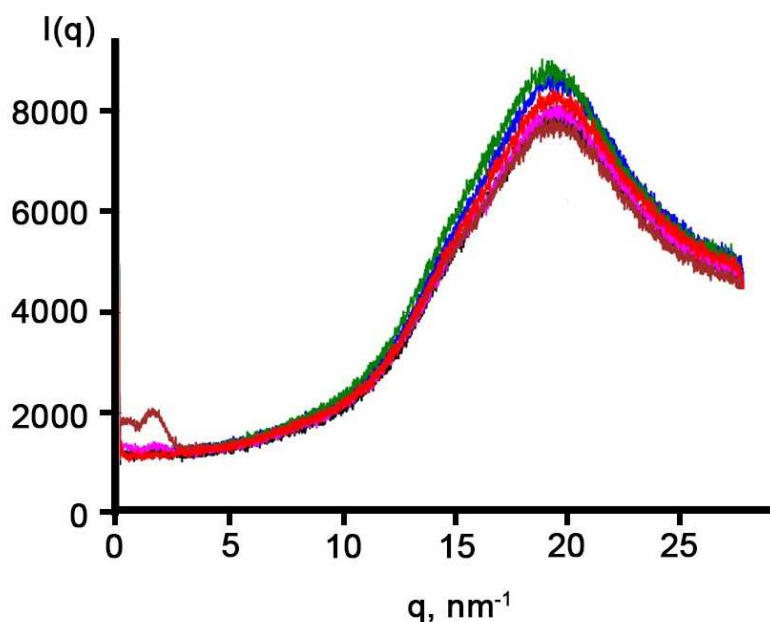


Figure 6. SAXS and broad-angle X-ray scattering data from micellar solution of SDS and water, the mode of linear collimation of the cross-section beam  $20 \times 0.3 \text{ mm}^2$  ( $\text{CuK}\alpha$ ,  $\alpha = 0.154 \text{ nm}$ ). The X-ray generator ID3003, 298K, exposure time 5 min. SDS concentrations (top down) - 0.01, 0.008, water, 0.02, 0.1 M.

A direct proof of the transformation of LDL  $\leftrightarrow$  HDL during LLPT was obtained by X-ray scattering, which, in contrast to the method of neutron scattering, "feels" the change in the electronic system of water. In Figure 6 the X-ray spectra of water and SDS solutions with concentrations greater than  $\text{CMC}_1$  are presented in the whole range available for diffractometer SAXSess Anton Paar<sup>42</sup>  $q=0.03\text{-}28 \text{ nm}^{-1}$ . The functions  $I(q)$  of the solutions have three peaks with maximum positions  $q=0.6, 1.5, \text{ and } 19 \text{ nm}^{-1}$ . The first peak corresponds to the distance between micelles. It seems visually that the functions  $I(q)$  for solutions with concentrations less 0.03 M do not have this peak. Therefore, it can be assumed that the interaction between micelles does not affect the diffraction pattern in 0.01 M SDS solution. The second peak reflects the presence of micelles in the solutions. It appears sharply at SDS concentration 0.1 M, when the equilibrium HDL  $\leftrightarrow$  HDL is completely shifted towards HDL ( $\text{CMC}_2$ ). Diffraction in the region about  $q=1.5 \text{ nm}^{-1}$  provides information about micelles structure. The third peak of broad-angle X-ray in the region  $q=15\text{-}28 \text{ nm}^{-1}$  corresponds to the picture in the near order of water. This peak is present in all functions  $I(q)$  of water and solutions.

In the first approximation, the small-angle and broad-angle X-ray scattering spectra can be considered as rows of Bragg peaks. Then the location of their maxima indicates the distance between the ordered aggregates of particles  $d_{\text{Bragg}}$ . According to the Bragg law:

$$d_{\text{Bragg}} = \frac{2\pi}{q_{\text{peak}}} \quad (3)$$

Using the equation (3) and the values of three peaks  $q_{\text{peak}}$ , the values of parameters  $d_{\text{Bragg}}$  can be estimated. The estimated parameters  $d_{\text{Bragg}}$  can be interpreted as the diameter of micelles – 4.2 nm, the distance between micelles – 10.5 nm and the distance O...O of molecular pair in the first coordination shell of water – 0.33 nm, which depends on the SDS concentration.<sup>43</sup> According to different data, the radial distribution function O...O has the maximum in the range from 0.28 up to 0.35 nm.<sup>44</sup> This region corresponds to the scattering by LDL and HDL clusters and by clusters formed around SDS molecules and micelles. As it can be seen from the equation (4), the function  $I(q)$  depends on the following parameters:

$$\frac{d\Sigma(q)}{d\Omega} = I(q) = I_0 N \rho^2 V^2 P(q), \quad (4)$$

where  $I_0$  is the device constant,  $N$  is the number of particles,  $\rho$  is the scattering-length density of water,  $V$  is the volume of scattering particle,  $P(q)$  is the form factor of the particle. The values of scattering-length density are equal to the following:  $\rho_{\text{water}} = 9.54 \cdot 10^{-6} \text{ \AA}^{-2}$ ,  $\rho_{\text{HDL}} = 11.16 \cdot 10^{-6} \text{ \AA}^{-2}$ ,  $\rho_{\text{LDL}} = 8.96 \cdot 10^{-6} \text{ \AA}^{-2}$ . If in the area of  $\text{CMC}_1$  the function  $I(q)$  depended only on the concentration of water, then we would have observed gradual decrease of  $I(q)$  with concentration of water as with SDS concentrations 0.02, 0.03, 0.1 M (Figure 6). However, the intensity of curve  $I(q)$  for  $q = 19 \text{ nm}^{-1}$  at SDS concentrations 0.008 and 0.01 M is greater than that of pure water (Figure 7). Therefore, in the area of  $\text{CMC}_1$  the electron density of clusters changes. It increases because HDL clusters appear around the micelles. We explain this phenomenon by the shift of the equilibrium  $\text{LDL} \leftrightarrow \text{HDL}$  towards HDL in the process of polyamorphous transition (Figure 3). For concentrations greater than 0.02 M, the increase in the content of HDL is compensates no more the decrease of  $I(q)$  due to the decrease of water content in the solution.

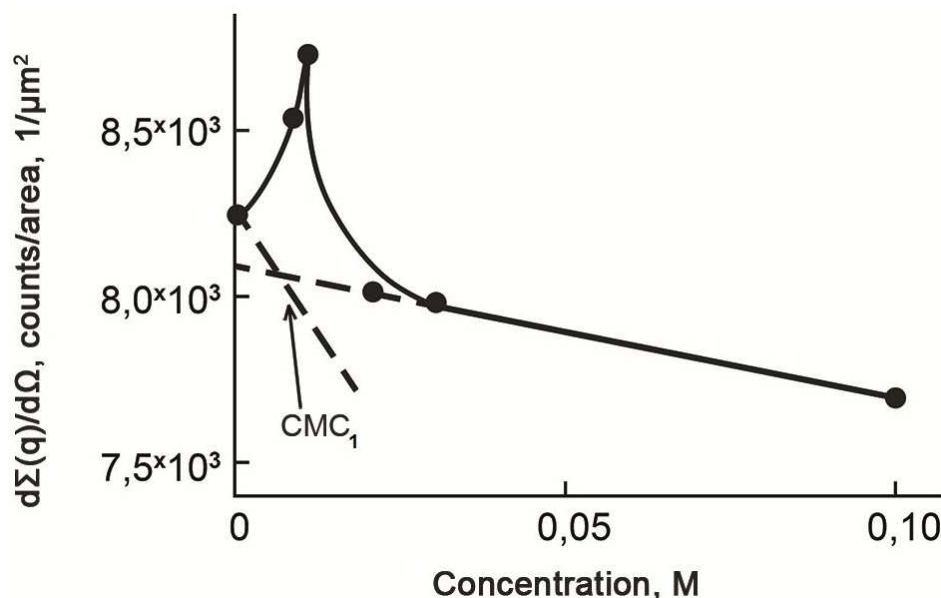


Figure 7. The dependence  $I(q)$  for  $q = 19 \text{ nm}^{-1}$  on the SDS concentration. Strokes illustrates a hypothetical straight line connecting  $I(q)$  of water with  $I(q)$   $\text{CMC}_1$  without  $\rho^2$  influence.

In our spectroscopic studies of structural characteristics of aqueous solutions of SDS in the process of micellization in SDS concentration range from  $1 \cdot 10^{-4} \text{ M}$  to  $3.5 \cdot 10^{-2} \text{ M}$ , we detected a sharp polyamorphous

transition in the ensemble of water clusters with high and low density at the time of micellization, which is confirmed by the results of application of the method of multidimensional curve resolution.<sup>45</sup> Namely, using the parameter  $\chi_{21} = I(\nu_2)/I(\nu_1)$ ,<sup>46,47</sup> equaled to the ratio of the intensities of high-frequency and low-frequency regions of the OH valence band, LLPT in the Raman spectrum of SDS solutions (Figure 8) was observed in a more narrow range of concentrations (Figure 7). The sharp shift of the balance in the ensemble of clusters from LDL to HDL occurs when the SDS concentration changes from  $4 \cdot 10^{-3}$  M to  $6 \cdot 10^{-3}$  M, reaching the maximum number of HDL clusters at the concentration of  $6 \cdot 10^{-3}$  M. With concentration of SDS increasing from  $6 \cdot 10^{-3}$  M to  $8 \cdot 10^{-3}$  M, the fraction of LDL decreases, and that of HDL increases (Figure 3). At the concentration of 0.05 M, the equilibrium between the number of LDL and HDL clusters establishes. Therefore, one can assume that in the process of LLPT, multi-parameter change of water properties occurs.

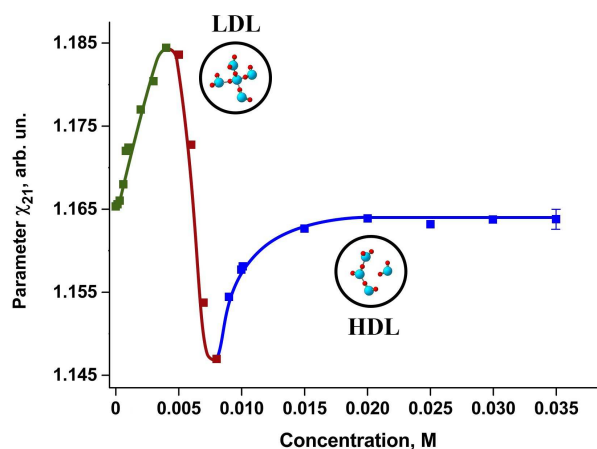


Figure 8. Change of  $\chi_{21} = I(\nu_2)/I(\nu_1)$  parameter (which is equal to the ratio of the intensities of high-frequency and low-frequency regions of the OH valence band) depending on SDS concentration.<sup>45</sup>

Thus, the experimental data confirm the theoretical conclusions and analysis, and they are consistent with recent experimental studies of water. In micellar aqueous solutions of surfactant and hydrotrops, the electron density of the water molecules changes at the length of about 0.3 nm. This is a direct experimental evidence of existence of LLPT between HDL and LDL. Water properties change in different in the LLPT zone depending on the method of research. The average concentration of transition corresponds to the concentration of formation of spherical micelles. It is between  $CPMC$  and  $CMC_2$ .

### 2.3. LLPT transition depending on the size of surfactants molecules.

Starting with s-heptylisothiuronium chloride, the shape of  $pH(\lg(x_2))$  changes.<sup>12</sup> Figure 4 shows that for this function of s-heptylisothiuronium chloride one can distinguish one particular point. We identify it with binodal. For C7 it coincides with  $CMC_1$  of this surfactant (Figure 1). Using function of  $pH(\lg(x_2))$  for each member of a homological series of ATC we obtained the dependence of the logarithm of the concentration of the specific points lying on the binodal on  $n$  (Figure 1, 5-5). The dependence  $\lg(CPMC(n))$  is s-shaped character. This dependence allows to draw a conclusion that the nature of LLPT depends not only on the number of small systems of water (concentration of ATC), but also on their size. There is a kind of discrete LLPT on binodal. In addition, the ensemble of small systems of water has stable and unstable states on binodal. It is possible to suppose by the s-shaped curve (Figure 1) that LLPT on binodal evolves from stable state of C2-C4 through unstable states of C5-C6 to a new stable state C7-C12.

It is logical to assume that every stable state meets its small systems. Lower organic electrolytes and hydrocarbons with  $n < 5$  form a crystalline clathrates with water.<sup>48</sup> From this we can conclude that clathrate structure of water corresponds to the tangent of the slope of the straight  $\lg(CPMC(n))$  of ATC with  $n < 5$ , i.e. hydrophobic ion of ATC is located in the cavities of tetrahedral network of H-bonds of water LDL.

In thermodynamics of hydrates formation the term "pressure of hydrate dissociation" is used, which should be comprehended as the minimum pressure of hydrocarbon, under which the clathrate still keeps thermodynamic stability. Similarly, for lower ATC the CPMC (Figure 5) should be understood as the concentration at which the "clathrate" of lower ATC still keeps its stability in solution. At further increase of the concentration a water structure near ATC begins to change. In the solution of ATC fluctuations of concentration begin to form, the maximum of these fluctuations will be on extension of  $\lg(CMC_1)$  of higher ATC (Figure 1, 6-6). Such conclusion can be drawn as the result of comparison of phase diagram of ATC with phase diagram of alcohols,<sup>22</sup> with levels of fluctuations of lower sodium alkanoates concentrations.<sup>49</sup>

If the nature of the small system near methylene group in solution similar to that in the clathrate that the proportional dependence should be between  $\lg CPMC$  and  $T_{melt}$  of crystalline hydrates of the another

homological series linked to the ATC. This dependence is observed, for example, between  $lgCPMC$  of ATC and  $T_{melt}$  of clathrates of alkanoates.<sup>12</sup>

With increasing chain length  $T_{melt}$  of clathrates of tetrabutylammonium alkanoates decreases. It may be assumed that with increasing chain length, a new type of the hydrate shell forms around hydrocarbon groups. For such process it is necessary the increase of not only the chain length, but also the concentration of ATC. The result of comparison of the increasing concentration of binodal of the ATC C7 - C12 with that of C2-C6 allows to assume that the hydrate shell of surfactants differs from the hydrate shell of clathrate type. During hydrophobic interaction small cations act on water like to the temperature decrease, and large cations act on water like to the temperature increase because they participate in hydrophobic interaction.<sup>50</sup>

To clarify the mechanism of hydrophobic hydration on binodal we consider a change of the apparent molal volume during substitution of hydrogen atom in hydrocarbon by the functional group of amphiphile ( $\Delta V_x^0$ ).<sup>51</sup> Hydrophilic groups in homologous series of amphiphiles undergo hydrophobic hydration under the influence of hydrophobic group. Therefore their values of  $\Delta V_x^0$  are much less their van der Waals volumes: -  $NH_3^+Cl^-$  15.4 ml/mole;  $-COO^-Na^+$  7 ml/mole. With increasing chain length the values of  $\Delta V_x^0$  of sodium carboxylates and alkylammonium chloride decrease and reach the limit values for C7. For the first surfactants the value of  $\Delta V_x^0$  equals to 7.8 ml/mole, for the second - 2.4 ml/mol, this corresponds to Figure 1. Hydrophilic group C7 is extremely hydrophobic as compared with C2-C6. The sign of the charge of hydrophilic group influence on change of hydration. As it can be seen, formation of the structure of LDL is more favorably near cationic amphiphiles. Therefore, it can be made the conclusion about the preferred orientation of oxygen of the water molecules in the structure of LDL relatively to the surface of hydrocarbon group, which stabilizes this structure on binodal. Apparently, in the ATC C7-C12 on binodal near hydrophilic group, from LDL a stable structure of "stocking" is formed. Water in the first hydrate layer of hydrophilic group does not participate in hydrophobic hydration and polyamorphic transitions. It is closed by the "stocking", which belongs to small system. The values of energies of water molecules interaction in the first hydrate layer and in the "stocking" differ by the order of magnitude. During LLPT the "stocking", apparently, is gradually changing. This phenomenon may explain the nature of chiral properties of the micellar solutions in the field of LLPT.<sup>52</sup>

Starting with the ATC C7 (Figure 1), binodal and spinodal of surfactant do not coincide with each other. When 0.1 M of NaCl is added in solutions of sodium alkylsulfates, spinodal shifts to binodal and they become parallel to binodal of alkanes,<sup>53</sup> nonionic amphiphiles. In these conditions, i.e. at the adding 0.1 M NaCl, cylindrical micelles are formed on binodal of DDS. Therefore, it is possible to assume that the lengthiness of LLPT is observed due to dissociation of the ionic surfactants.

Thus, in dependence on the sizes of amphiphiles molecules and their concentration on binodal the small systems of water molecules of different nature are formed. Their chemical potentials are equal to the chemical potentials of small systems of amphiphiles, i.e. molecules, consisting of several methylene groups. When the sizes of amphiphiles change there is peculiar "discrete phase transition" on binodal. It is transition from LDL with small slowdown of re-orientation of water molecules for hydrotropes with  $n < 4$ , with average slowdown for hydrotropes with  $n = 5, 6$  to a large slowdown for the typical surfactants with  $n > 7$ . The structure of small systems of water on binodal determines the type of LLPT over concentration. In the solutions of ATC with  $n = 2-4$  when the concentration increases the "melting" clathrate structures is observed. In result of this the microdecomposition with manifestation of concentration fluctuations is observed. In the solutions of ATC with  $n = 7-12$  the structure of LDL with large slowdown of reorientation of water molecules in small system gradually transfers into the structure of HDL with formation of bistable spherical micelles. ATC with  $n = 7$  has a critical volume. Taking into account the hydrophilic group the size of C7 is equal to the size of undecane approximately. The formation of bistable micelles begins from solutions of s-heptylisonium chloride.

#### 2.4. Features of polymorphous transition and self-organization of amphiphiles

In the region of dilute solutions up to binodal the formation of ion associate between ions of surfactants with opposite signs finishes. The average ionic coefficient of activity  $\gamma_{\pm}$  loses its physical meaning because the association of ion pairs occurs not due to electrostatic interaction, but due to hydrophobic interaction, i.e. it is accompanied by LLPT.<sup>9</sup> In the area of LLPT  $\lg \gamma_{\pm}$  obeys the linear law.

$$\lg \gamma_{\pm} = \lg \gamma_{\pm}^0 + K_{\gamma} x, \quad (5)$$

where  $\gamma_{\pm}^0$  characterizes the contribution of interionic interaction and it is the true ionic activity coefficient.

$K_{\gamma}$  is the parameter of activity coefficient of Sechenov,  $x$  - concentration of amphiphile.

In the study of solubilization in solutions of surfactants, hydrotropes with hydrocarbons in the area of LLPT the cooperative effect was discovered. That is directly proportional dependence between the Gibbs energy of aggregation and the total length of the chain of partners in intermolecular interaction in the processes of micellization, solubilization, hydrotropy, condensation of two organic ions with opposite charges. For the manifestation of the cooperative effect the certain conditions should be preserved. They are the following: preservation of the same mechanism of hydrophobic interaction, hydrogen bonding, the donor-acceptor interaction, uniformity of hydrocarbon groups in amphiphile and hydrocarbon. The cooperative effect is due to the fact that in the area of LLPT self-organization of amphiphiles is determined only by the water activity<sup>8</sup> or  $V/\beta_T$  of water.

We have shown that LLPT forms two different structures of micelles of amphiphiles C7-C12: contact ( $\Delta G_{\text{CH}_2(\text{M})}^0 = -3.7 \text{ kJ}\cdot\text{mole}^{-1}$ ) and hydrated ( $\Delta G_{\text{CH}_2(\text{M})}^0 = -1.4 \text{ kJ}\cdot\text{mole}^{-1}$ ), where  $\Delta G_{\text{CH}_2(\text{M})}^0$  is increment of standard Gibbs energy of micellization (Figure 2).<sup>26</sup> Water does not increase the intermolecular interaction of methylene groups of surfactants in the micelle in comparison with the dispersion interaction in the liquid hydrocarbon. In other words, the contribution of water in intermolecular interaction takes place in two structures of micelles and leads to the total effect of the thermodynamic functions with their statistical weight  $\Delta G_{\text{CH}_2(\text{M})}^0 = -3.0 \text{ kJ}\cdot\text{mole}^{-1}$ ,  $\Delta H_{\text{CH}_2(\text{M})}^0 = 1.0 \text{ kJ}\cdot\text{mole}^{-1}$ ,  $T\Delta S_{\text{CH}_2(\text{M})}^0 = 4.0 \text{ kJ}\cdot\text{mole}^{-1}$ . Water "groups" molecules of surfactants in two types of micelles. At the same time it changes its intermolecular interaction by means of LLPT thus, to coexist with micelles, hydrocarbon groups of which interact in a particular way:  $\Delta G_{\text{CH}_2}^0$  of this interaction is equal to  $\Delta G_{\text{CH}_2}^0$  of dispersion interactions in liquid hydrocarbon. Each of the two structures of micelles is realized in result of LLPT.

Thus, micelles are bistable. They have two minima of Gibbs energy of micellization on the methylene group ( $\Delta G_{\text{CH}_2}^0 = -3.0 \text{ kJ}\cdot\text{mole}^{-1}$ ,  $-0.7 \text{ kJ}\cdot\text{mole}^{-1}$ ) and one maximum ( $\Delta G_{\text{CH}_2}^0 = +0.7 \text{ kJ}\cdot\text{mole}^{-1}$ ) when the methylene group is in the water. The ensemble of water clusters can have two states: or in the form of HDL, or in the form of LDL with their statistical weight. The activation energies of the transition of methylene



groups from two stable states through the unstable state are equal to 1.4 and 3.7 kJ mol<sup>-1</sup>, accordingly. These values were obtained when micellization was tested by hydrophobic probe - molecules of gaseous hydrocarbons in the process of solubilization.<sup>30,54</sup> The duality of structure of spherical micelles of alkylammonium chloride is proved by us with help of method of NMR.<sup>55</sup>

We found the hysteresis during solubilization in two solubilization series: n-hydrocarbons - sodium dodecyl sulphate and alkyl sulphates of sodium – propane.<sup>54</sup> The hysteresis of properties is observed in bistable systems.<sup>56</sup> It is absent in the solutions of hydrotropes of tetraalkylammonium bromides that do not form micelles, but increase the solubility of hydrocarbons in water (Figure 9). The hysteresis of conductivity was observed in solutions of surfactants near the point Craft.<sup>57</sup>

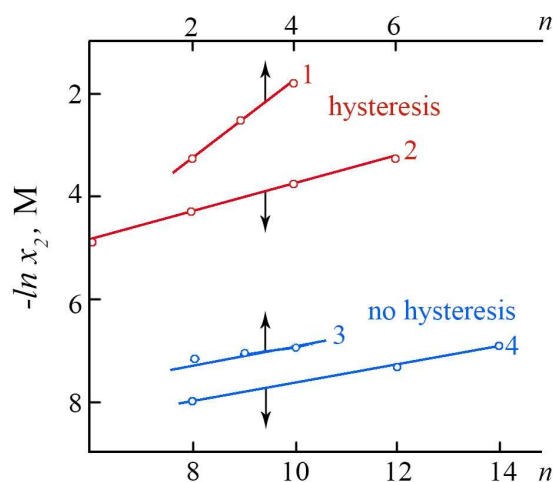


Figure 9. Hysteresis during solubilization in two solubilization series. The dependence of the natural logarithm of hydrocarbons solubilization on the number of carbon atoms (n) in alkyl group of alkylsulfate sodium and tetraalkylammonium bromides at 25°C. 1 - hydrocarbons C2-C4 in solutions of sodium dodecyl sulfate, 2 - propane in solutions of sodium alkyl sulphates C6-C10 (hysteresis - two different values tangent in two the solubilization series), 3 - hydrocarbon in solutions of tetrabutylammonium bromide, 4 - propane in solutions of the tetraalkylammonium bromides (no hysteresis – one values tangent in two the solubilization series).

1  
2  
3  
4  
5  
6  
7  
8  
9  
10  
11  
12  
13  
14  
15  
16  
17  
18  
19  
20  
21  
22  
23  
24  
25  
26  
27  
28  
29  
30  
31  
32  
33  
34  
35  
36  
37  
38  
39  
40  
41  
42  
43  
44  
45  
46  
47  
48  
49  
50  
51  
52  
53  
54  
55  
56  
57  
58  
59  
60

In the kinetic theory, the elementary stage of SDS micellization is presented as equilibrium between the molecule and micellar aggregate.<sup>58</sup> Rate constant of the direct reaction  $\kappa_+ = 1.2 \cdot 10^9 \text{ l} \cdot \text{mole}^{-1} \cdot \text{s}^{-1}$ , and the rate constant of the inverse reaction  $\kappa_- = 1 \cdot 10^7 \text{ l} \cdot \text{mole}^{-1} \cdot \text{s}^{-1}$ . In the framework of our approach, it is assumed that the two rate constants obtained in experiments, correspond to two values of the Gibbs energy of activation in the transition between two states of a self-oscillating system. They can be calculated by the Arrhenius equation.<sup>13</sup> For SDS micelles,  $\Delta G$  are equal to -19.4 and -29.8  $\text{kJ} \cdot \text{mole}^{-1}$ , respectively. The difference between them (-10.4  $\text{kJ} \cdot \text{mole}^{-1}$ ) is less than  $\Delta G$  for the H-bond in the water (-5  $\text{kJ} \cdot \text{mole}^{-1}$ ). Therefore, small systems overcome the energy barrier and oscillate. The fluctuations of the intensity of fluorescence spectrum of zinc protoporphyrin dimethyl ether in the area of 580 nm was observed in SDS micellar solutions.<sup>59</sup> Fluorescence in the solution was excited by radiation with 410 nm wavelength. In the ethanol solutions of the same substances at the same concentrations, fluctuations in the intensity of fluorescence were no observed.

Mutual influence and compromise between hydrophobic and hydrophilic hydration allows one to compare hydrophobic hydration of SDS and hydrocarbons. A measure of comparison of the size of their small systems can be isobaric heat capacity  $c_p^0$ .<sup>60</sup> Analysis of experimental data on  $\Delta c_p^0$  allows drawing the following conclusions. Changes in  $\Delta c_p^0$  depend on the structure and state of water molecules, and do not depend on the state of aggregation of hydrocarbons, amphiphiles. Positive values of  $\Delta c_p^0$  are due to hydrophobic hydration, and negative ones are due to hydrophilic hydration. They give independent contribution to  $\Delta c_p^0$ . Comparing  $\Delta c_p^0$  of SDS (547  $\text{J K}^{-1} \text{ mole}^{-1}$ ) and that of liquid hydrocarbons, we obtain that small water systems around SDS molecules and around octane molecules are the same, as for octane  $\Delta c_p^0 = 541 \text{ J K}^{-1} \text{ mole}^{-1}$ . Thermal effects of dissolution of crystal SDS<sup>41</sup> and of liquid octane ( $\Delta H_s^0 = 2 \text{ kJ mole}^{-1}$ ) are the same also.<sup>61</sup> Therefore, similar to hydrocarbons it is possible to calculate LLPT enthalpy for SDS using  $\Delta H_s^0$ . Calculation yields 4.6  $\text{kJ mole}^{-1}$  for enthalpy and 15.44  $\text{kJ mole}^{-1} \text{ K}^{-1}$  for the entropy. These values are equal to the corresponding values for the process of ice melting approximately.

Thus, in the LLPT zone, the ion coefficient of activity of the surfactant is constant. For Gibbs energy of hydrophobic interactions, cooperative effect is observed. Micelles are bistable, so hysteresis of properties and oscillations can be found in solutions. Micellization, like that of hydrocarbons, is accompanied by LLPT

with enthalpy  $4.6 \text{ kJ mole}^{-1}$ . Enthalpy and entropy of LLPT in aqueous solutions of surfactants and hydrocarbons, in spite of different nature, are equal to those of phase transition of crystallization/melting of ice. This is so because, when dissolved, surfactant and hydrocarbons before binodal affect the ensemble of small systems of water like decrease of temperature, and during micellization - like increase of temperature.

## 2.5. Instabilities of systems in LLPT region

Similarly to phase separation in an open system, LLPT of micelle-forming amphiphiles is accompanied by instabilities of the thermodynamic system.<sup>62</sup>

Surface tension of freshly prepared aqueous solutions of SDS with increasing concentration from 0.001 to 0.003 mole/l does not decrease, as at other concentrations, but increases (Figure 10). In 15 minutes after setting of the adsorption equilibrium, the strange concentration area disappears, and gradual decrease of surface tension is observed instead.

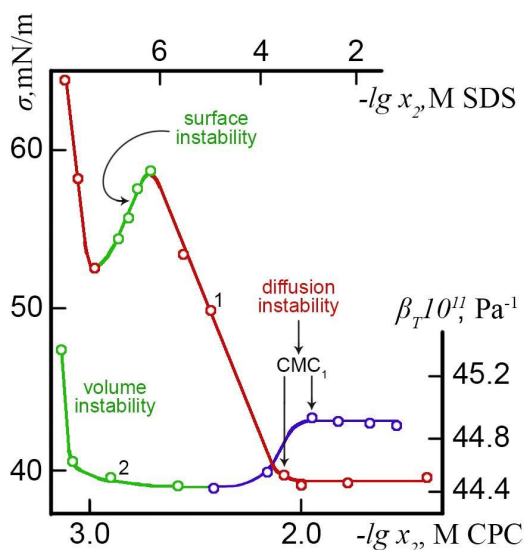


Figure 10. Instabilities of systems in the LLPT region. The isotherm of surface tension of aqueous solutions of sodium dodecyl sulfate immediately after preparation (1), isothermal compressibility of water solutions of N-cetylpyridinium chloride (CPC) (2) at 298 K.

The observed paradox, or surface mechanical instability, is apparently caused by complex kinetics of adsorption layer formation at concentrations of sodium alkyl sulphates, corresponding to binodal. On the

binodal, there compete adsorption, which reaches its maximum value, and formation of SDS dimers. Adsorption is accompanied by decrease in the surface tension, and association of SDS into dimers tends to reduce the amount of SDS on the surface and, therefore, to increase the surface tension.

In aqueous solutions of surfactants water behaves as clean water under effective internal pressure.<sup>63</sup> With increasing concentration of surfactants, internal water pressure increases. Figure 10 shows the dependence of  $\beta_T$  of water solutions of N-cetylpyridinium chloride on its concentration.<sup>49</sup> As can be seen,  $\beta_T$  decreases to binodal (minimum  $\beta_T(-\lg(x_2))$ ), what corresponds to loosening of the solution with increase of the internal pressure  $(\partial\beta_T/\partial x)_{T,P} < 0$ . Inequality corresponds to manifestation of volume mechanical instability. Before CMC<sub>1</sub> (spinodal)  $\beta_T(-\lg(x_2))$  increases, what corresponds to densifying of the solution.

If CMC<sub>1</sub> is considered to be equal to true surfactant solubility, then it belongs to binodal. However, micellization in the area of CMC<sub>1</sub> is accompanied by a discontinuity of mutual diffusion coefficient  $D$ .<sup>64</sup> The coefficient of mutual diffusion of SDS and water in the area of CMC<sub>1</sub> sharply decreases, and then increases. Such behavior of the coefficient of mutual diffusion at concentrations about CMC<sub>1</sub> is analogous to approximation to the spinodal of decomposition solutions. As micelles are formed, that is, microphases emerge and  $(\partial D/\partial x_2) > 0$  is observed in the zone of micellization, then one can assume manifestation of thermodynamic (diffusion) instability. This conclusion can be checked by experimental coefficients of SDS activity  $\gamma$  in the zone of micellization. The mutual diffusion coefficient is given by the expression.<sup>65</sup>

$$D = k_B T B (1 + \partial \ln \gamma / \partial \ln x_2), \quad (6)$$

where  $B$  is the coefficient of mobility of amphiphile (always positive). The expression in brackets in equation (6) determines whether the diffusion coefficient is positive, negative or equal to zero. The calculation by experimental  $\gamma$  data for SDS at CMC<sub>1</sub> for the relation in brackets gives the value (-0.93).<sup>66</sup> Taking into account the experimental error, it means that  $D$  is very close to zero, i.e. that CMC<sub>1</sub> belongs to the spinodal.

Thus, due to the structure of a closed thermodynamic system, surface and volume mechanical instabilities and diffusion instability are observed in it.

### 3. PRACTICAL APPLICATIONS OF THE LLPT CONCEPT

We used peculiarities of LLPT for practical application (Figure 11). If water-soluble polymers or hydrotropes are present in the solution together with hydrocarbon, then in the triple system water - hydrocarbons – hydrotropes, due to the cooperative effect, polymer and hydrotrop become surfactant, with its inherent property to lower the surface tension at the boundary of the two phases and to solubilize hydrocarbons. So instead of expensive typical surfactants, for tertiary oil production from depleted wells is possible to use water-soluble polymers and hydrotropes.<sup>49</sup> The authors<sup>67</sup> used hydrotropic waste to increase oil production, using the idea of our patent.

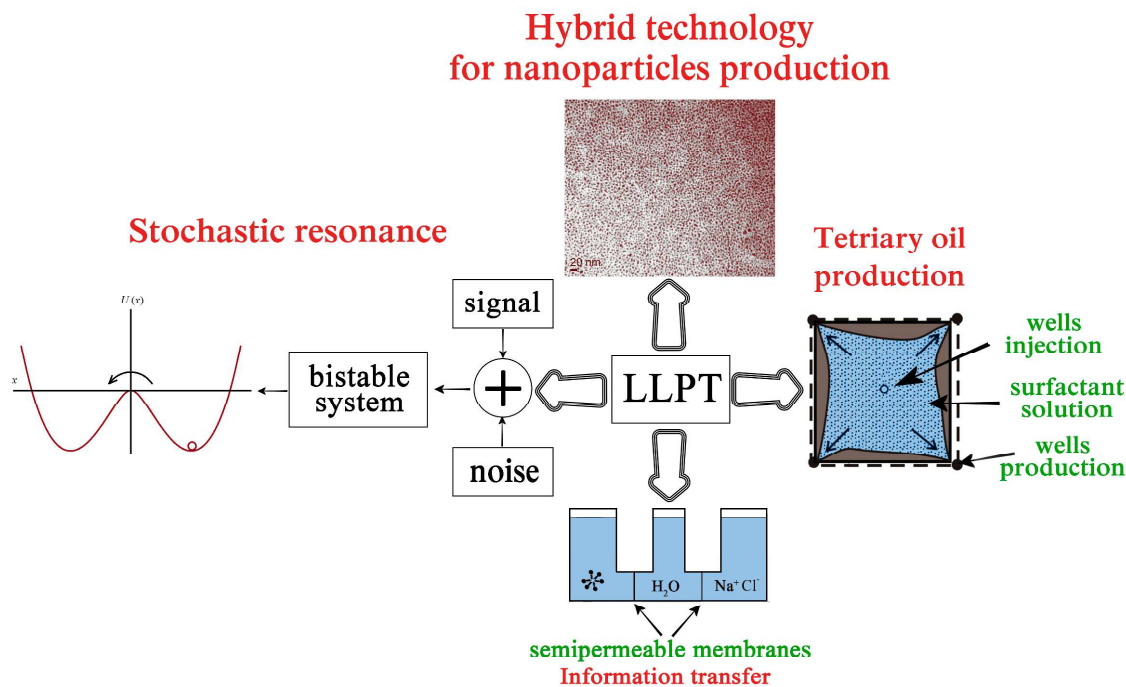


Figure 11. Use of LLPT properties for practical applications. Explanation of the technology is in the text.

Structural-phase transformation of lipids in aqueous solutions are an important element of reading/writing information at the level of synaptic membranes of brain. Change of the area of hysteresis has been recorded under the action of biological substances that are added directly into the solution of lipids.<sup>68</sup> According to the LLPT concept, structural-phase transformations in water solutions of lipids are due to the influence of additives on the structure of water. The latter may affect  $CMC_1$  even through the layer of water that separates the solution of the additive from the lipid solution by membranes permeable only to water molecules (Figure 11). When the ratio of concentrations of NaCl and SDS equals 1:1 (mole),  $CMC_1$  is reduced compared with the presence of SDS in two vessels.<sup>49</sup>

1  
2  
3  
4  
5  
6  
7  
8  
9  
10  
11  
12  
13  
14  
15  
16  
17  
18  
19  
20  
21  
22  
23  
24  
25  
26  
27  
28  
29  
30  
31  
32  
33  
34  
35  
36  
37  
38  
39  
40  
41  
42  
43  
44  
45  
46  
47  
48  
49  
50  
51  
52  
53  
54  
55  
56  
57  
58  
59  
60

In accordance with hybrid technology, with the help of ion flotation or flotoextraction, one can efficiently and economically separate and concentrate different elements. Next, the precursor consisting of the surfactant and ion is reduced to nanoparticles of metals, or nanoparticles of hydroxides and oxides are obtained by action of alkali in direct micelles (nanoreactors) of the same surfactants used for flotoextraction. Surfactants are regenerated, and nanoparticles are used to get nanomaterials.<sup>69,70</sup>

The effect of stochastic resonance determines a group of phenomena, in which the response of bistable systems (micelles) to a weak external signal significantly increases with the intensity of noise in the system.<sup>59,71</sup> In this case, integral characteristics at the output of the system such as gain and signal-to-noise ratio, have a clearly pronounced maximum at a certain optimal noise level.

#### 4. CONCLUDING REMARKS AND OUTLOOK

In this review, we have attempted to summarize and to develop the concept of LLPT for aqueous solutions of hydrocarbons, alcohols, surfactants and hydrotropes. The following conclusions can be formulated to summarize.

1. LLPT accompanies the fluctuations of concentration of hydrocarbons, alcohols, hydrotropes, surfactant micelle formation. Hydrophobic interaction should be understood as the total contribution of the intermolecular interaction water/water, hydrocarbon/water and hydrocarbon/hydrocarbon in the process of LLPT.

2. Properties of LLPT are determined by the properties of water, by the structure of hydrocarbons, amphiphiles and by their concentration. With increasing molecular sizes and concentration before binodal in excess water the amphiphiles affect water like temperature decrease, and shift the equilibrium LDL  $\leftrightarrow$  HDL towards LDL. The second binodal is achieved when the lack of water for LLPT shifts the equilibrium towards HDL. CMC<sub>1</sub> coincides with the midpoint of LLPT or with spinodal. Due to the special properties of LLPT (self-oscillations), the system overcomes the spinodal. Addition of an inorganic electrolyte to the solutions of surfactants causes convergence of two binodals and the spinodal.

3. LLPT is determined using the activity of water, Raman spectroscopy, NMR, X-ray scattering of water, hydrolysis of ATC. With a decrease in the concentration of water (increasing the surfactant

concentration), the electron density of water on the scale of 0.3 nm increases. This is a direct evidence of shift of the equilibrium towards HDL, i.e. of existence of LLPT.

4. Due to LLPT, the ion activity coefficient of ionic surfactants loses its meaning; the cooperative effect, bistability, hysteresis, self-oscillations, fluctuations of extensive properties; surface, volumetric and thermodynamic instabilities of the system are observed. The value of the changes of enthalpy and entropy of LLPT is approximately equal to the energy of melting/crystallization of ice, and they are caused by the effect of volume of the dissolved molecules on LLPT.

The LLPT concept does not contradict universally recognized experimental data. In the equation  $\Delta G_M^s = (1 + K_d)RT \ln(CMC_1)$ , bistability of micelles has been taken into account: the first term of the equations corresponds to the contribution of pseudophase A to the Gibbs energy, and the second – to the contribution of associate B. Already known theories of the kinetics of micelle formation still cannot exactly interpret the correspondence of relaxation processes and structures in the process of micellization, so a new interpretation of the experimental kinetic parameters is possible. The LLPT concept explains how it is possible to get over spinodal, and embeds micellization into the general theory of phase separation. Hydrocarbon groups of amphiphiles before binodal influence water like decreasing temperature. After binodal, hydrocarbon groups influence water like increasing temperature. The studied LLPT are in the same row: in supercooled water, nanoporous bodies, supercooled solutions of polyols, protein solutions.

For the development of the concept it is necessary to develop new methods of LLPT identification, to investigate the self-oscillatory properties, hysteresis and bistability of micelles, the structure of water in the transition region. It is interesting to find the connection between self-oscillatory properties in the bulk and on the surface of the solution.

Although LLPT in supercooled water is intensively investigated, it is not paid sufficient attention at normal temperatures in water solutions of inorganic electrolytes, non-electrolytes, hydrotropes, surfactants. The authors hope that this article will attract attention to our concept of LLPT and it will stimulate LLPT research in these substances.

ACKNOWLEDGEMENT

We thank Peter M. Worsch (Anton Paar) and Alex Chekadanov (Southwest State University) for help with the SAXS measurements. This work was supported by the RF Ministry of Education and Science through the federal targeted program *The Scientists and Science Educators of Innovative Russia*, project no. P848.

## References

1. Anisimov, M. A. Cold and Supercooled Water: a Novel Supercritical Fluid Solvent. *Russ. J. Phys. Chem B* **2012**, *6*, 1-7.
2. Sun, Z. R.; Sun G.; Chen Y. X.; LiMei X. U. Liquid-liquid phase transition in water. *Sci China - Phys. Mech. Astron.* **2014**, *57*, 810–818.
3. Huang, C.; Wikfeldt, K. T.; Tokushima, T.; Nordlund, D.; Harada, Y.; Bergmann, U.; Niebuhr, M.; Weiss, T. M.; Horikawa, Y.; Leetmaa, M.; Ljungberg, M; Takahashi, O.; Lenz, A.; Ojamäe, L.; Lyubartsev, A. P.; Shin, S.; Pettersson, L. G. M.; Nilsson, A. The Inhomogeneous Structure of Water at Ambient Conditions. *Proc. Natl. Acad. Sci. U.S.A.* **2009**, *106*, 15214-15218.
4. Clark, G. N. I.; Cappab, C. D.; Smith, J. D.; Saykally, R. J.; Head-Gordon, T. The Structure of Ambient Water. *Mol. Phys.* **2010**, *108*, 1415-1433.
5. Zhang, Y.; Faraone, A.; Kamitakahara, W. A.; Liu, K.-H.; Mou, C.-Y.; Leao, J.B.; Chang, S.; Chen, S.-H. Density Hysteresis of Heavy Water Confined in a Nanoporous Silica Matrix. *Proc. Natl. Acad. Sci. U.S.A.* **2011**, *108*, 12206-12211.
6. Schiro, G.; Fomina, M.; Cupane, A. Protein Dynamical Transition vs. Liquid-Liquid Phase Transition in Protein Hydration Water. *J. Chem. Phys.* **2013**, *139*, 121102-121104.
7. Murata, C.-I.; Tanaka, H. Liquid-liquid Transition without Macroscopic Phase Separation in a Water-Glycerol Mixture. *Nature Material.* **2012**, *11*, 436-443.
8. Biddle, J. W.; Holten, V.; Anisimov, M. A. Behavior of Supercooled Aqueous Solutions Stemming from Hidden Liquid-Liquid Transition in Water. *arXiv cond-mat. soft 1404.2627v2.* **2014**, 1-12.
9. Mirgorod, Yu. A. Cooperative Self-Organization in Aqueous Solutions. *Russ. J. General Chem.* **1994**, *64*, 189-192.



- 1  
2  
3  
4  
5  
6  
7  
8  
9  
10  
11  
12  
13  
14  
15  
16  
17  
18  
19  
20  
21  
22  
23  
24  
25  
26  
27  
28  
29  
30  
31  
32  
33  
34  
35  
36  
37  
38  
39  
40  
41  
42  
43  
44  
45  
46  
47  
48  
49  
50  
51  
52  
53  
54  
55  
56  
57  
58  
59  
60
10. Murata, C.-I.C.; Tanaka, H. General Nature of Liquid–Liquid Transition in Aqueous Organic Solutions. *Nature Commun.* **2013**, *4*, 2844-2851.
  11. Robinson, G. W.; Cho, C. H. Role of Hydration Water in Protein Unfolding. *Biophys. J.* **1999**, *77*, 3311-3318.
  12. Mirgorod, Yu. A. Liquid-Liquid Phase Transition in Aqueous Solutions of n-Hydrocarbons and Amphiphiles. *Techn. Phys. Lett.* **2010**, *36*, 892-894.
  13. Mirgorod, Yu. A. Investigating the Dependence of Polymorphic Liquid–Liquid Transitions on the Concentration of Amphiphiles in Water. *Rus. J. Phys. Chem. A* **2015**, *89*, 10–15.
  14. Nagarajan, R. One Hundred Years of Micelles: Evolution of the Theory of Micellization. In *Surfactant Science and Technology: Retrospects and Prospects*, L. Romsted (Ed.), Taylor and Francis, New York, **2013**.
  15. Hammouda, B. Temperature Effect on the Nanostructure of SDS Micelles in Water. *J. R. of the Nation. Ins. of Stand. and Tech.* **2013**, *118*, 151-167.
  16. Kim, H.-Un; Lim, K.-Hee. Sizes and Structures of Micelles of Cationic Octadecyl Trimethyl Ammonium Chloride and Anionic Ammonium Dodecyl Sulfate Surfactants in Aqueous Solutions. *Bull. Korean Chem. Soc.* **2004**, *25*, 382-388.
  17. Mirgorod, Yu. A.; Efimova, N. A. Contact and Water-Separated Hydrophobic Interactions in Micellar Solutions of Surfactants. *Russ. J. Phys. Chem.* **2007**, *81*, 1665-1668.
  18. Bernardino, K.; de Mauro, A. F. Aggregation Thermodynamics of Sodium Octanoate Micelles Studied by Means of Molecular Dynamics Simulations. *J. Chem. Phys. B* **2013**, *117*, 7324-7334.
  19. Rharbi, Y.; Bechthold, N.; Landfester, K.; Salzman, A.; Winnik, M. A. Solute Exchange in Synperonic Surfactant Micelles. *Langmuir* **2003**, *19* (1), 10–17.
  20. Toyota, T.; Uchiyama, K.; Kimura, T.; Nomoto, T.; Fujinami, M. Effects of Surfactants and Electrolytes on Chemical Oscillation at a Water/Nitrobenzene Interface Investigated by Quasi-Elastic Laser Scattering Method. *Analytical Sciences* **2013**, *29*, 911-917.
  21. Gao, J.; Wang, L.; Yang, W.; Yan, F. Electrical Potential Oscillation in an Anionic Surfactant System with Barbitone in Octanol as an Oil Phase. *J. Iranian Chem. Soc.* **2005**, *2*, 71-77.

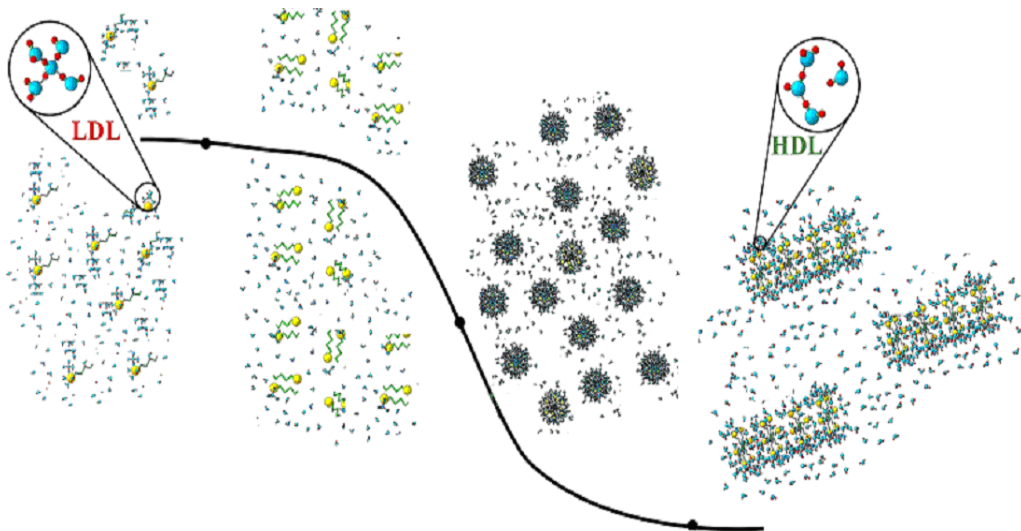
- 1  
2  
3  
4  
5  
6  
7  
8  
9  
10  
11  
12  
13  
14  
15  
16  
17  
18  
19  
20  
21  
22  
23  
24  
25  
26  
27  
28  
29  
30  
31  
32  
33  
34  
35  
36  
37  
38  
39  
40  
41  
42  
43  
44  
45  
46  
47  
48  
49  
50  
51  
52  
53  
54  
55  
56  
57  
58  
59  
60
22. Mirgorod Yu. A. Polymorphic Transitions in Binary Systems n-Hydrocarbons-Water, n-Alcohols-Water. *Russ. J. Phys. Chem.* **2014**, *88* (8), 1312-1316.
23. Subramanian, D.; Boughter, C. T.; Klauda, J. B.; Hammouda, B.; Anisimov, M. A. Mesoscale Inhomogeneities in Aqueous Solutions of Small Amphiphilic Molecules. *Faraday Discuss.* **2013**, *167*, 217-238.
24. Petersen, C.; Tielrooij, A. K.-J.; Bakker, H. J. Strong Temperature Dependence of Water Reorientation in Hydrophobic Hydration Shells. *J. Chem. Phys.* **2009**, *130*, 214511-214516.
25. Mirgorod, Yu. A. The Solubilities of Propylbenzene and Hexane in Water as Functions of Temperature. *Rus. J. Phys. Chem.* **2002**, *76*, 1608-1611.
26. Mirgorod, Yu. A. Thermodynamic Analysis of the Dynamic Structure of Micellar Solutions of Sodium Alkylsulfates. *J. Struct. Chem.* **2008**, *49*, 889-893.
27. Chandler, D. Interfaces and the Driving Force of Hydrophobic Assembly. *Nature* **2005**, *437*, 640-647.
28. Mirgorod, Yu. A. Thermodynamic Analysis of the Structure of Aqueous Solutions of C12-C18 Hydrocarbons. *J. Struct. Chem.* **2009**, *50*, 456-460.
29. MCMilan, P. F. Polyamorphic Transformation in Liquid and Glasses. *J. Mater. Chem.* **2004**, *14*, 1506-1512.
30. Mirgorod, Yu. A. Methylene Group Increments of the Gibbs Energy of Solution of Hydrocarbons in Water and Aqueous Micellar Solutions of Surface-Active Substances. *Rus. J. Phys. Chem.* **2001**, *75*, 352-355.
31. Hill, T. *Thermodynamic of small system*. N-Y-A., Benjamin, **1963**.
32. Mirgorod, Yu. A. Change in the Structure of Water as a Function of Chain Length of Diphilic Molecules and Hydrocarbons. *J. Struct. Chem.* **1986**, *27*, 418-423.
33. Mirgorod, Yu. A. Structure of Dilute Aqueous Solutions of Sodium Dodecylsulfate. *J. Struct. Chem.* **1991**, *32*, 853-856.
34. Mirgorod, Yu. A.; Chepenko, A. I. Investigation of Submicelle Formation in Aqueous Solutions of Alkylammonium Chlorides and Sodium Alkylsulfates by Use of Anionic Hydrophobic Probe. *Colloid J.* **1981**, *43*, 963-966.

- 1  
2  
3  
4  
5  
6  
7  
8  
9  
10  
11  
12  
13  
14  
15  
16  
17  
18  
19  
20  
21  
22  
23  
24  
25  
26  
27  
28  
29  
30  
31  
32  
33  
34  
35  
36  
37  
38  
39  
40  
41  
42  
43  
44  
45  
46  
47  
48  
49  
50  
51  
52  
53  
54  
55  
56  
57  
58  
59  
60
35. Poole, P. H.; Sciortino, F.; Essmann, U.; Stanley, H. E. Phase Behavior of Metastable Water. *Nature* **1992**, *360*, 324–328.
36. Gonzalez-Perez, A.; Czapkiewicz, J.; Ruso, Z.M.; Rodriguez, Z. R. Temperature Dependence of Second Critical Micelle Concentration of Dodecyltrimethylbenzylammonium Bromide in Aqueous Solution. *Colloid. Polym. Sci.* **2004**, *282*, 1169-1173.
37. Mirgorod, Yu. A. Degree of Cooperativity During Micelle Formation in Aqueous Solutions of Ionogenic Surfactants. *Colloid J.* **1992**, *54*, 861-863.
38. Lindman, B.; Puyal, M.-C.; Kamenka, H. J.; Brun, B.; Gunnarson, G. Micelle Formation of Anionic and Cationic Surfactant from Fourier Transform Hydrogen-1 and Lithium-7. Nuclear Magnetic Resonance and Tracer Self-Diffusion studies. *J. Phys. Chem.* **1982**, *86*, 1702-1711.
39. Danielson, I.; Rosenholm, J. B.; Stenius, P.; Basklund, S. Liotropic Mesomorphism and Aggregation in Surfactant Systems. *Progr. Colloid. and Polym. Sci.* **1976**, *61*, 1-11.
40. Khripun, M. K.; Gubanov, V. A.; Efimov, V. F.; Brettske, E. V. Study of the Surface Activity of the Ammonium Salt of Perfluoro-2-Methyl-3-Hexanoic Acid by Proton Relaxation. *Colloid. J.* **1982**, *44*, 380-384.
41. Batov, D.V.; Kartsev, B. H.; Shtykova, L. S.; Shtykov, S.N. Calorimetric Study of Aqueous Solutions of Sodium Dodecylsulfate and Triton X-100 at 298.15 K. *Chem. Chem. Tech. (Russ)*. **2003**, *46*, 80-84.
42. Schnablegger H., Singh Y. The SAXS Guide. Austria. Anton Paar. 2011.
43. Wernet, P.; Nordlund, D.; Bergmann, U.; Cavalleri, M.; Odelius, M.; Ogasawara, H.; Näslund, L.A.; Hirsch, T.K.; Ojamäe, L.; Glatzel, J.P.S.; Pettersson, L.G.M.; Nilsson, A. The Structure of the First Coordination Shell in Liquid Water. *Science* **2004**, *304*, 995-999.
44. Wang, J.; Román-Pérez, G.; Soler, J. M.; Artacho, E.; Fernández-Serra, M-V. Density, Structure, and Dynamics of Water: The Effect of Van der Waals Interactions. *J. Chem. Phys.* **2011**, *134*, 024516.
45. Dolenko, T. A.; Burikov, S.A.; Dolenko, S.A.; Efitorov, A. O.; Mirgorod, Yu. A. Raman Spectroscopy of Micellization-Induced Liquid-Liquid Fluctuations in Sodium Dodecyl Sulfate Aqueous Solutions. *J. Mol. Liq.* **2015**, *204*, 44-49.

- 1  
2  
3  
4  
5  
6  
7  
8  
9  
10  
11  
12  
13  
14  
15  
16  
17  
18  
19  
20  
21  
22  
23  
24  
25  
26  
27  
28  
29  
30  
31  
32  
33  
34  
35  
36  
37  
38  
39  
40  
41  
42  
43  
44  
45  
46  
47  
48  
49  
50  
51  
52  
53  
54  
55  
56  
57  
58  
59  
60
46. Gogolinskaia (Dolenko), T.A.; Patsaeva, S.V.; Fadeev, V.V. The Regularities of Change of the 3100-3700  $\text{cm}^{-1}$  Band of Water Raman Scattering in Salt Aqueous Solutions. *Doklady Akademii Nauk SSSR* **1986**, *290* (5), 1099-1103.
47. Dolenko, T. A.; Burikov, S. A.; Rosenholm, J. M.; Shenderova, O. A.; Vlasov, I. I. Diamond-Water Coupling Effects in Raman and Photoluminescence of Nanodiamond Colloidal Suspensions. *J. Phys. Chem. C* **2012**, *116*, 24314-24319.
48. Goncharuk, V. V.; Smirnov, V. N.; Syroeshkin, A. V.; Malyrenko, V. V. Clusters and Gigantic Heterophase Water Clusters. *J. Water Chem. Techn.* **2007**, *29*, 1-8.
49. Mirgorod, Yu. A. *Aqueous Hydrocarbon Systems in Science and Engineering*, State Tekhn. Inst., **2001**.
50. Huang, N.; Schlesinger, D.; Nordlund, D.; Huang, C.; Tyliczszak, T.; Weiss, T. M.; Acremann, Yv.; Pettersson, L. G. M.; Nilsson, A. Microscopic Probing of the Size Dependence in Hydrophobic Solvation. *J. Chem. Phys.* **2012**, *136*, 074507.
51. Mirgorod, Yu. A. Mechanisms of Hydrophobic Interaction of Benzene with Alkylammonium Bromides in Aqueous Solutions. *Colloid. J.* **1981**, *43*, 708-712.
52. Rusanov, A. I.; Nekrasov, A. G. One More Extreme Near the Critical Micelle Concentration: Optical Activity. *Langmuir* **2010**, *26*, 13767-13769.
53. Mirgorod, Yu. A. Concentration-Chain Length Diagrams and the Structure of Aqueous Solutions of Diphilic Molecules. *J. Struct. Chem.* **1983**, *24*, 93-99.
54. Mirgorod, Yu. A. Solubility of Ethane, Propane, and Butane in Aqueous Solutions of Sodium Dodecyl Sulfate. *Russ. J. General Chem.* **2005**, *75*, 31-33.
55. Mirgorod, Yu. A.; Postnikov, E. B.; Borshch, N. A.  $^{13}\text{C}$  NMR Investigation of the Structure of Alkylammonium Chloride Micelles. *J. Struct. Chem.* **2010**, *51*, 1111-1118.
56. Ball, R.; Haymet, A. D. J. Bistability and Hysteresis in Self-Assembling Micelle Systems: Phenomenology and Deterministic Dynamics. *Phys. Chem. Chem. Phys.* **2001**, *3*, 4753-4761.
57. Manojlovic, J. Z. The Krafft Temperature of Surfactant Solutions. *Thermal Science* **2012**, *16*, 631-640.
58. Jonsson, B.; Lindman, B.; Holmberg, K.; Kronberg, B. *Surfactants and Polymers in Aqueous Solution*, first ed., John Wiley & Sons, London, **1998**.

- 1  
2  
3  
4  
5  
6  
7  
8  
9  
10  
11  
12  
13  
14  
15  
16  
17  
18  
19  
20  
21  
22  
23  
24  
25  
26  
27  
28  
29  
30  
31  
32  
33  
34  
35  
36  
37  
38  
39  
40  
41  
42  
43  
44  
45  
46  
47  
48  
49  
50  
51  
52  
53  
54  
55  
56  
57  
58  
59  
60
59. Mirgorod, Yu. A. Oscillations of Fluorescence Intensity in Sodium Dodecylsulfate Aqueous-Solutions with Protonoporphine (IX) Dimethyl Ether-Zinc Complexes. *J. General Chem.* **1995**, *65*, 155-156.
60. Graziano, G.; Barone, G. Group Additivity Analysis of the Heat Capacity Changes Associated with the Dissolution into Water of Different Organic Compounds. *J. Am. Chem. Soc.* **1996**, *118*, 1831-1835.
61. Tonopoulos, C.; Wilson, G. M. Thermodynamic Analysis of the Mutual Solubilities of Normal Alkanes and Water. *Fluid Phase Equilibrium* **1999**, *156*, 21-33.
62. Mirgorod, Yu. A. Development of Internal Instability with the Concentration of Amphiphilic Electrolytes in Aqueous Solutions. *Russ. J. Phys. Chem.* **1988**, *54*, 1089-1091.
63. Lyubimov, S. L.; Churagulov, B. R.; Baranov, A. N. The Rule of Tamman-Gibson and General Regularities of Variation with Pressure of the Partial Molar Volumes of Electrolytes in Aqueous Solutions. *Russ. J. Phys. Chem.* **1997**, *71*, 642-647.
64. Siderius, A.; Kehl, S.K.; Leaist, D. G. Surfactant Diffusion Near Critical Micelle Concentrations. *J. Solut. Chem.* **2002**, *31*, 607-625.
65. Nakagaki, M. *Physical chemistry membranes*, Mir, Moscow, **1991** [In Russian].
66. Sasaki, T.; Hattori, M.; Sasaki, J.; Nukina, K. Studies of Aqueous Sodium Dodecyl Sulfate Solutions by Activity Measurements. *Bull. Chem. Soc. Japan.* **1975**, *48*, 1397-1403.
67. Kudasheva, F. H.; Badikova, A. D.; Mussina, A. M.; Mutallim, I. Y. Compositions for Oil-Swiping on the Base of Petrochemistry Wastes. *Neftegazov. Delo* **2010**, *1*. [In Russian].
68. Kuzurman, P. A.; Arkhipova, G. V. On the Structural and Molecular Nature of Mechanisms for Recording and Reading Information. *Biophysics* **2002**, *47*, 1049-1054.
69. Mirgorod, Yu. A.; Borshch, N. A.; Yurkov, G. Yu. Preparation of Nanomaterials from Aqueous Solutions Imitating the Hydrometallurgy Waste. *Rus. J. Appl. Chem.* **2011**, *84*, 1314-1318.
70. Mirgorod, Yu. A.; Borshch, N. A.; Fedosyuk, V. M. The Structure and Magnetic Properties of Cobalt Ferrite Nanoparticles Synthesized in a System of Direct Micelles of Amphiphiles by Means of Ion Flotoextraction. *Rus. J. Phys. Chem.* **2012**, *86*, 418-423.
71. Anishchenko, V. S.; Neiman, A. B.; Moss, F.; Shimansky-Geier, L. Stochastic Resonance: Noise-Enhanced Order. *Phys. Usp.* **1999**, *42*, 7-36.

1  
2  
3  
4  
5  
6  
7  
8  
9  
10  
11  
12  
13  
14  
15  
16  
17  
18  
19  
20  
21  
22  
23  
24  
25  
26  
27  
28  
29  
30  
31  
32  
33  
34  
35  
36  
37  
38  
39  
40  
41  
42  
43  
44  
45  
46  
47  
48  
49  
50  
51  
52  
53  
54  
55  
56  
57  
58  
59  
60



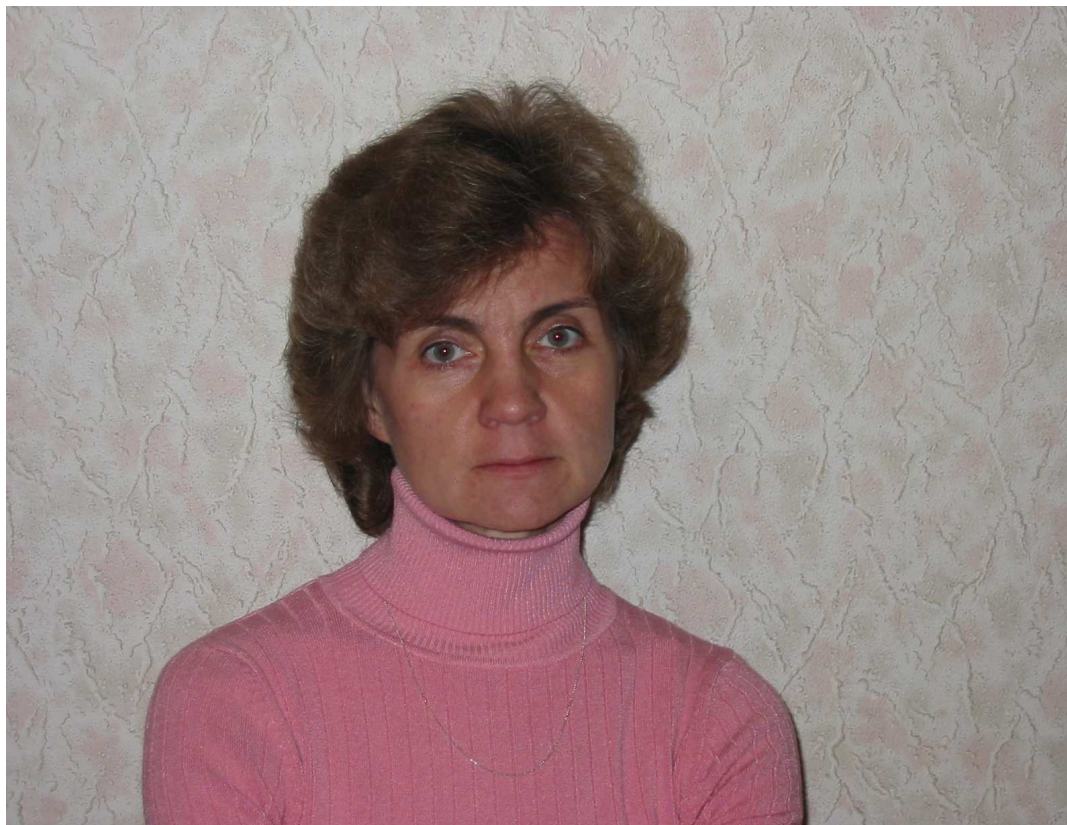
**Yuriy A. Mirgorod**

1 Yuriy A. Mirgorod received Engineer Diploma from Department of Chemical Engineering, Polytechnic  
2  
3  
4 Institute (Kharkov, the Ukraine) in 1962. In 1970, he received Ph.D. (Organic Chem.) from Kharkov  
5  
6 Polytechnic Institute. In 1993, he received Doctor of Science (Colloid Chem./Petrochem.) from Institute of  
7  
8 Petrochem., Academy of Science, the Ukraine. Now he is a full professor in the Department of Fundamental  
9  
10 Chemistry at Southwest State University (Kursk, Russia), and he is a leading researcher of the Regional Centre  
11  
12 of Nanotechnology. His current research interests are focused on the synthesis, physical and chemical properties  
13  
14 of surfactant and application in nanotechnology.  
15  
16  
17  
18  
19



1  
2  
3  
4  
5  
6  
7  
8  
9  
10  
11  
12  
13  
14  
15  
16  
17  
18  
19  
20  
21  
22  
23  
24  
25  
26  
27  
28  
29  
30  
31  
32  
33  
34  
35  
36  
37  
38  
39  
40  
41  
42  
43  
44  
45  
46  
47  
48  
49  
50  
51  
52  
53  
54  
55  
56  
57  
58  
59  
60

Tatiana A. Dolenko graduated *cum laude* in 1983 from Physical Department of M.V.Lomonosov Moscow State University (MSU). In 1987, she received PhD in physics and mathematics from MSU. Now she is a Senior research scientist at M.V.Lomonosov Moscow State University (Department of Physics). Since 2008, T.Dolenko is the Head of Group of laser spectroscopy of solutions of supramolecular compounds and nanostructures. She is the author of about 130 papers. Area of research: Raman and IR spectroscopy, aqueous solutions of supramolecular substances, colloidal solutions of nanoparticles, inverse problems, artificial neural networks.





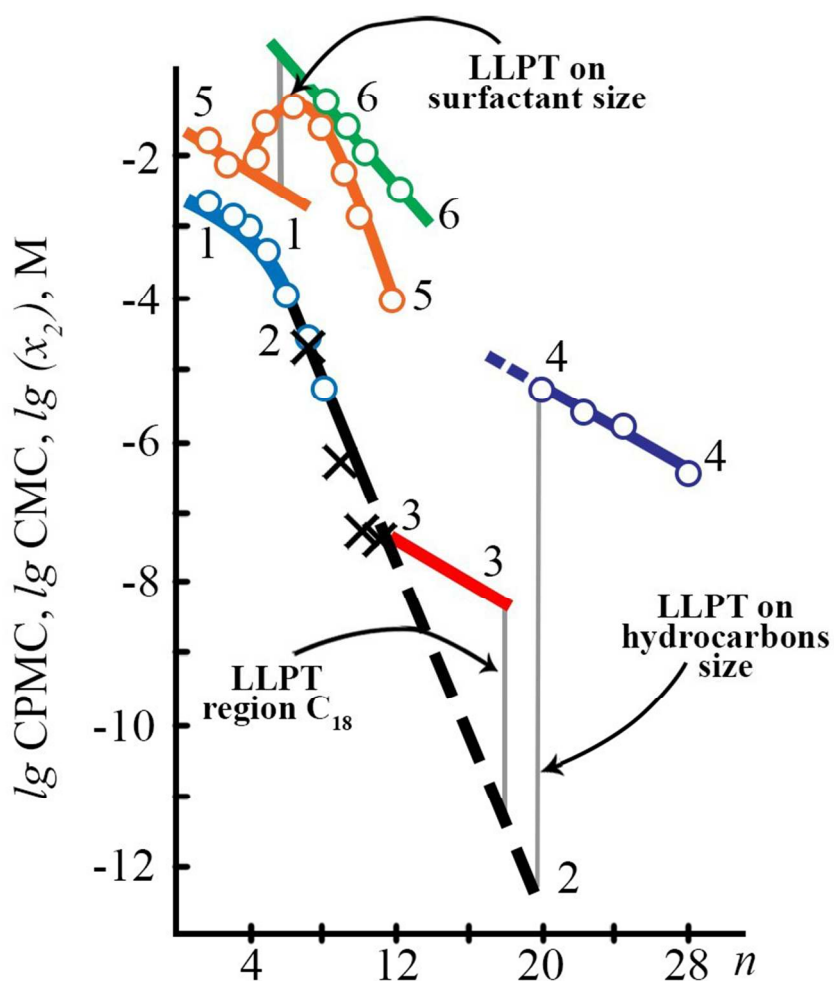


Figure 1. Phase diagrams of *n*-hydrocarbons and of *s*-alkylisothiuronium chlorides. 1,1 - solubility, binodal of gases of hydrocarbons C1-C4; 2,2 - solubility, binodal and spinodal of hydrocarbons; C5-C11; 3,3 - micellar solubility, spinodal of hydrocarbons C11-C18; 3,2- solubility, binodal of hydrocarbons C11-C18; 4,4 - micellar solubility, binodal of hydrocarbons C19-C28; 5,5 - critical pre-micelle concentration (CPMC), binodal of C2-C12 of *s*-alkylisothiuronium chlorides; 6,6 -  $\text{CMC}_1$ , spinodal of C7-C12 of *s*-alkylisothiuronium chlorides.

85x85mm (300 x 300 DPI)

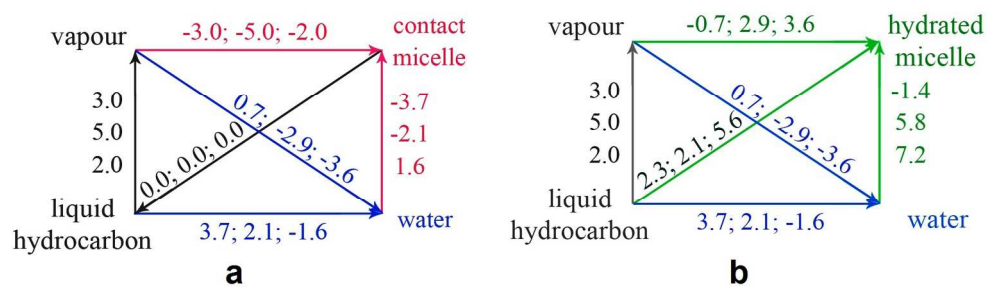


Figure 2. Thermodynamic cycles of  $\Delta G_{CH_2}^0$ ,  $\Delta H_{CH_2}^0$ ,  $T\Delta S_{CH_2}^0$  ( $\text{kJ}\cdot\text{mole}^{-1}$ ) of processes of dissolution in water, of evaporation, of hydrocarbon hydration, migration of hydrocarbon from vapour and water in micelles: contact hydrophobic (a) and hydrated hydrophobic (b) interaction.  
164x51mm (300 x 300 DPI)

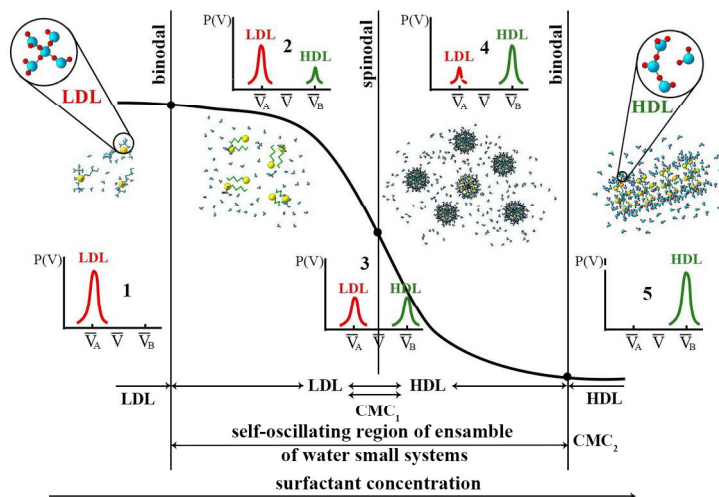


Figure 3. Polyamorphous transition in the ensemble of water small systems and self-organization of surfactant. Smooth change in the properties of water and self-oscillating region of water small systems between two binodal with increasing concentration of the amphiphile. 1 - the probability of volumes of water small system in the state A before the first binodal (CPMC); 2 - the probability of volumes of water small system in the state A and B between the first binodal and spinodal ( $CMC_1$ ), 3 - the probability of volumes of water small system in the state A and B on the spinodal ( $CMC_1$ ); 4 - the probability of volumes of water small systems in the state A and B between the spinodal and the second binodal ( $CMC_2$ ); 5 - the probability of volumes of water small system in the state B behind the second binodal ( $CMC_2$ ).

170x85mm (300 x 300 DPI)

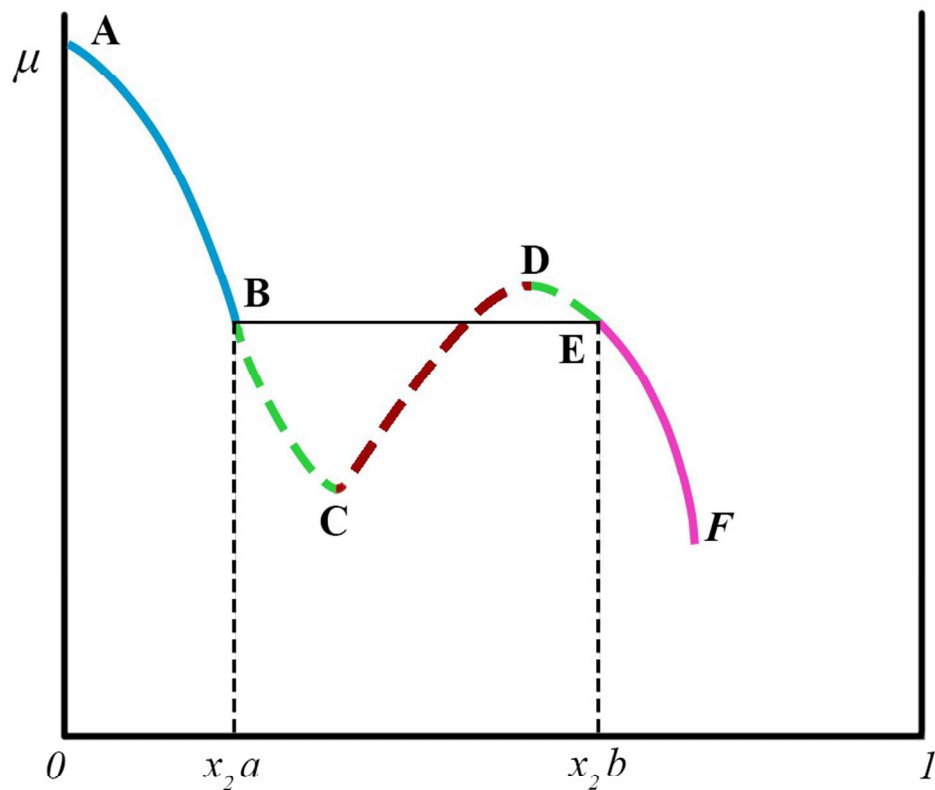


Figure 4. Dependence of chemical potential of one of the component a on system composition a+b in the framework of the general theory of phase separation. AB - single-phase state, EF-another single-phase state; BC, DE - metastable states, CD-unstable state, BE - two-phase state.  
85x85mm (300 x 300 DPI)

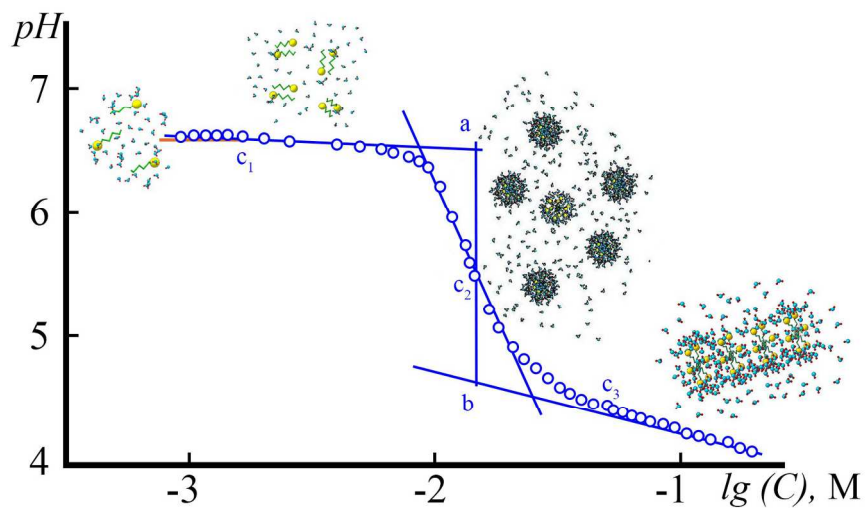


Figure 5 (a). Dependence of polyamorphous transition on the concentration of amphiphile. The dependence of pH on logarithm of the concentration of s-decylisothiuronium chloride in aqueous solution at 25°C.  $C_1$  is the beginning of the transition (the beginning of formation of pre-micelles),  $C_2$  is the middle of LL-transition ( $CMC_1$ ),  $C_3$  is the completion of transition ( $CMC_2$ ),  $ab$  is the "depth" of the transition.  
170x85mm (300 x 300 DPI)

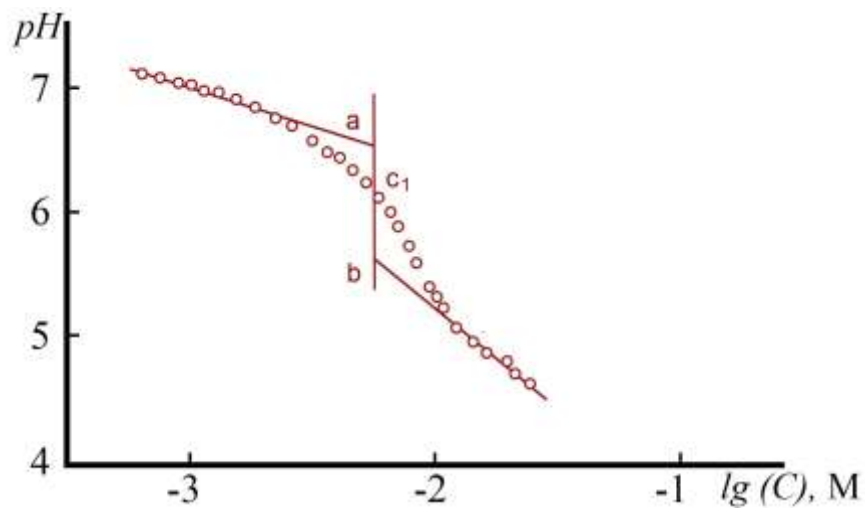


Figure 5 (b). Dependence of polyamorphous transition on the concentration of amphiphile. The dependence of pH on logarithm of the concentration of s-hexylisothiuronium chloride in aqueous solution at 25°C.  $C_1$  is the beginning of the transition (the beginning of formation of pre-micelles),  $C_2$  is the middle of LL-transition ( $CMC_1$ ),  $C_3$  is the completion of transition ( $CMC_2$ ), ab is the "depth" of the transition.  
170x85mm (300 x 300 DPI)

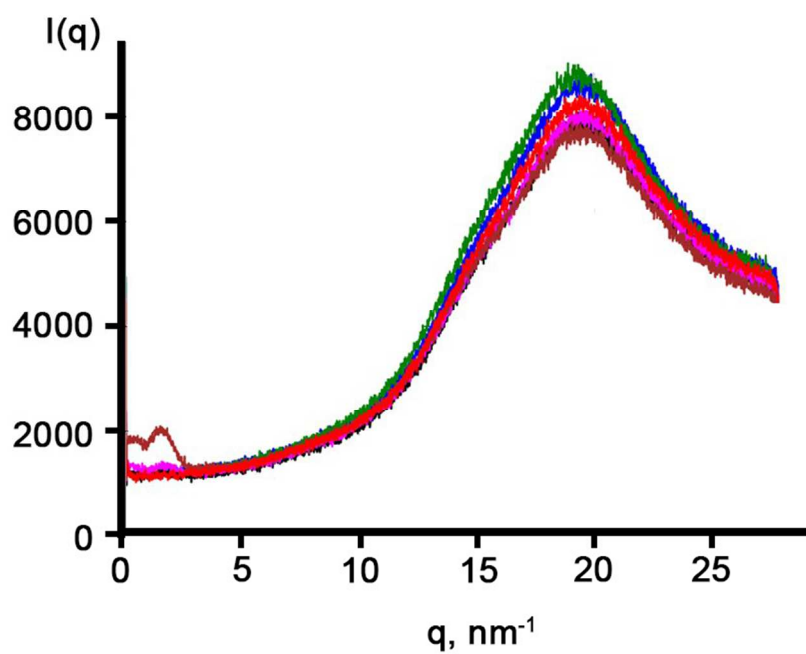


Figure 6. SAXS and Broad-Angle X-ray Scattering data from micellar solution of SDS and water, the mode of linear collimation of the cross-section beam  $20 \times 0.3 \text{ mm}^2$  ( $\text{CuK}\alpha$ ,  $\lambda = 0.154 \text{ nm}$ ). The X-ray generator ID3003, 298K, exposure time 5 min. SDS concentrations (top down) - 0.01, 0.008, water, 0.02, 0.1 M. 85x85mm (300 x 300 DPI)

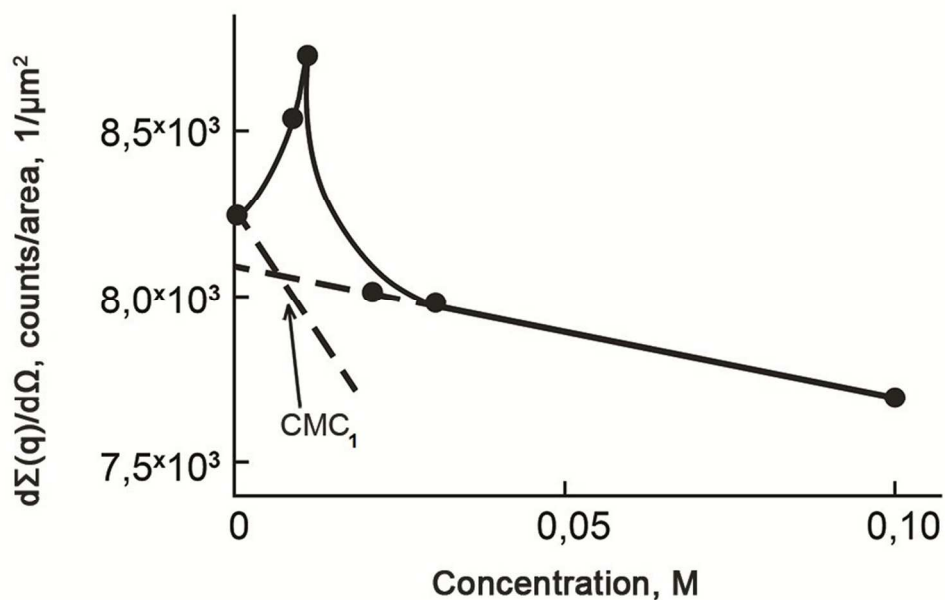


Figure 7. The dependence  $I(q)$  for  $q = 19 \text{ nm}^{-1}$  on the SDS concentration. Strokes illustrates a hypothetical straight line connecting  $I(q)$  of water with  $I(q)$   $\text{CMC}_1$  without  $\rho^2$  influence.  
85x85mm (300 x 300 DPI)



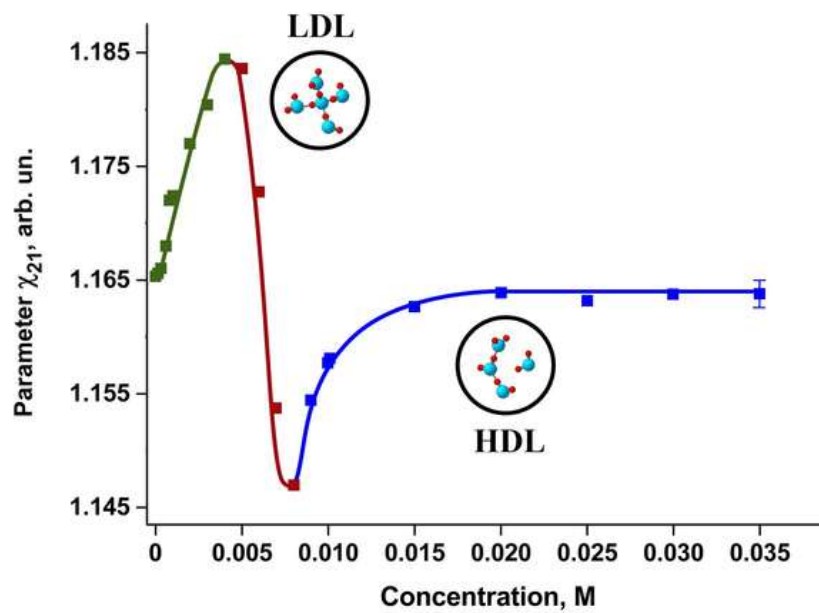


Figure 8. Change of  $\chi_{21} = I(v_2)/I(v_1)$  parameter (which is equal to the ratio of the intensities of high-frequency and low-frequency regions of the OH valence band) depending on SDS concentration.<sup>45</sup>  
59x41mm (300 x 300 DPI)

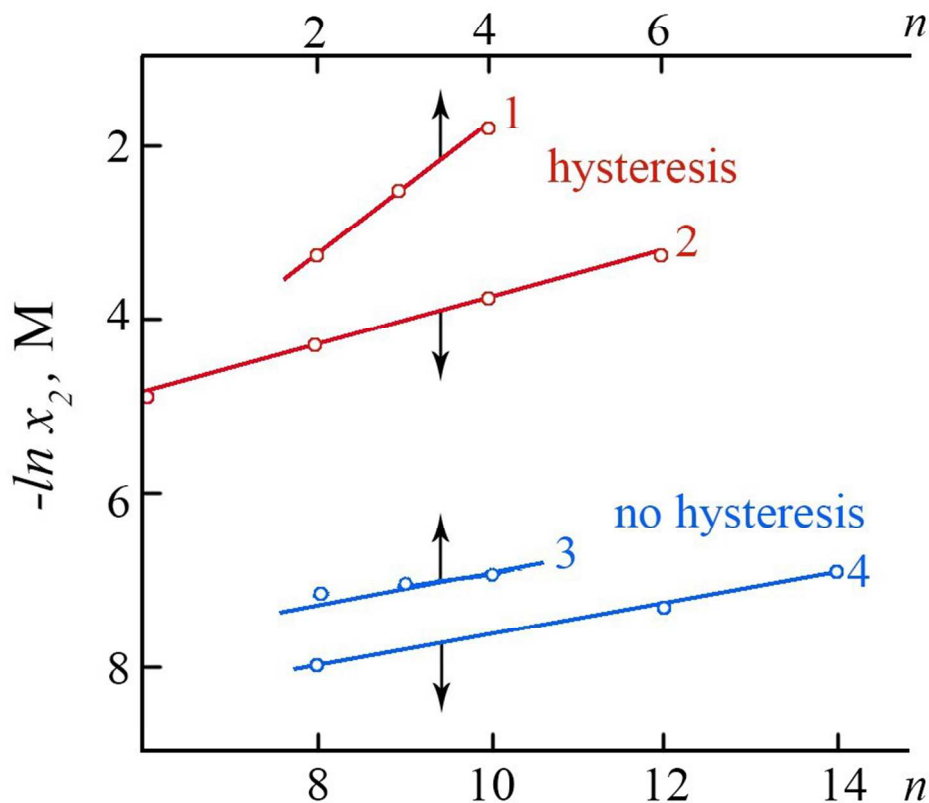


Figure 9. Hysteresis during solubilization in two solubilization series. The dependence of the natural logarithm of hydrocarbons solubilization on the number of carbon atoms ( $n$ ) in alkyl group of alkylsulfate sodium and tetraalkylammonium bromides at 25°C. 1 - hydrocarbons C2-C4 in solutions of sodium dodecyl sulfate, 2 - propane in solutions of sodium alkyl sulphates C6-C10 (hysteresis - two different values tangent in two the solubilization series), 3 - hydrocarbon in solutions of tetrabutylammonium bromide, 4 - propane in solutions of the tetraalkylammonium bromides (no hysteresis - one values tangent in two the solubilization series).

85x85mm (300 x 300 DPI)

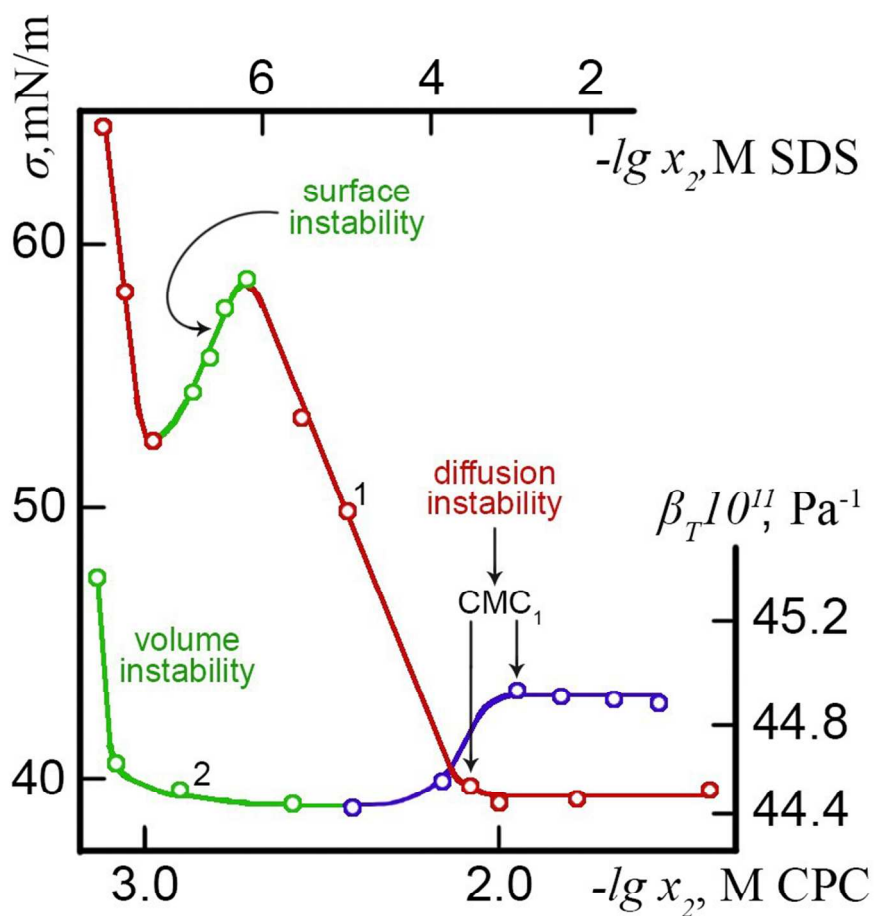


Figure 10. Instabilities of systems in the LLPT region. The isotherm of surface tension of aqueous solutions of sodium dodecyl sulfate immediately after preparation (1), isothermal compressibility of water solutions of N-cetylpyridinium chloride (CPC) (2) at 298 K.  
85x85mm (300 x 300 DPI)

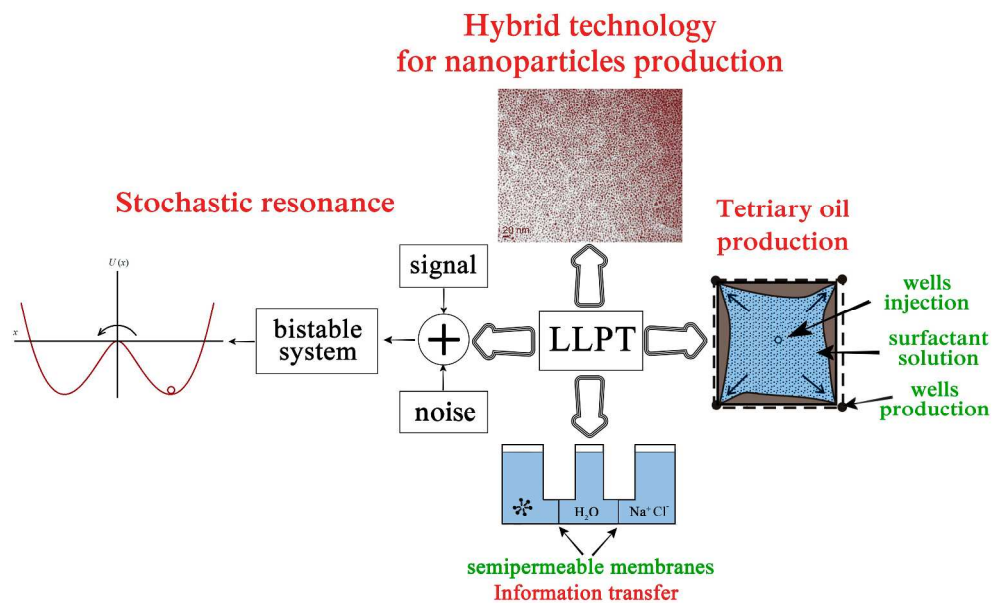
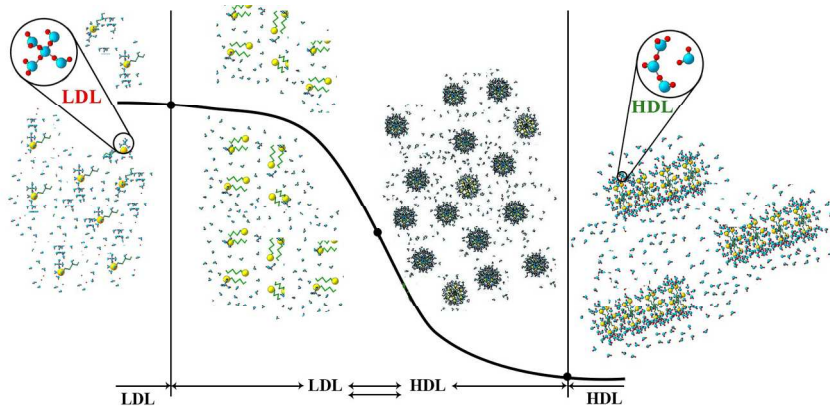


Figure 11. Use of LLPT properties for practical applications. Explanation of the technology is in the text.  
401x247mm (300 x 300 DPI)



Yu.A.Mirgorod, T.A.Dolenko. Liquid Polyamorphous Transition and Self-Organization in Aqueous Solutions of Ionic Surfactants  
170x85mm (300 x 300 DPI)